NBS REPORT
6728

FIRST QUARTERLY REPORT

to

National Aeronautics and Space Administration

on

Cryogenic Research and Development

for

Quarter Ending September 30, 1960

NBS

U. S. DEPARTMENT OF COMMERCE
NATIONAL BUREAU OF STANDARDS
BOULDER LABORATORIES
Boulder, Colorado

THE NATIONAL BUREAU OF STANDARDS

Functions and Activities

The functions of the National Bureau of Standards are set forth in the Act of Congress, March 3, 1901, as amended by Congress in Public Law 619, 1950. These include the development and maintenance of the national standards of measurement and the provision of means and methods for making measurements consistent with these standards: the determination of physical constants and properties of materials: the development of methods and instruments for testing materials, devices, and structures; advisory services to government agencies on scientific and technical problems: invention and development of devices to serve special needs of the Government; and the development of standard practices, codes, and specifications. The work includes basic and applied research, development, engineering, instrumentation, testing, evaluation, calibration services, and various consultation and information services. Research projects are also performed for other government agencies when the work relates to and supplements the basic program of the Bureau or when the Bureau's unique competence is required. The scope of activities is suggested by the listing of divisions and sections on the inside of the back cover.

Publications

The results of the Bureau's work take the form of either actual equipment and devices or published papers. These papers appear either in the Bureau's own series of publications or in the journals of professional and scientific societies. The Bureau itself publishes three periodicals available from the Government Printing Office: The Journal of Research, published in four separate sections, presents complete scientific and technical papers; the Technical News Bulletin presents summary and preliminary reports on work in progress; and Basic Radio Propagation Predictions provides data for determining the best frequencies to use for radio communications throughout the world. There are also five series of nonperiodical publications: Monographs, Applied Mathematics Series, Handbooks. Miscellaneous Publications, and Technical Notes.

Information on the Bureau's publications can be found in NBS Circular 460, Publications of the National Bureau of Standards ($1.25) and its Supplement ($1.50), available from the Superintendent of Documents, Government Printing Office, Washington 25, D.C.

NATIONAL BUREAU OF STANDARDS REPORT

NBS PROJECT		NBS REPORT
81410, 81420, and 81430	September 30, 1960	6728

FIRST QUARTERLY REPORT

to

National Aeronautics and Space Administration

on

Cryogenic Research and Development

for

Quarter Ending September 30, 1960

NBS

U. S. DEPARTMENT OF COMMERCE
NATIONAL BUREAU OF STANDARDS
BOULDER LABORATORIES
Boulder, Colorado

IMPORTANT NOTICE

NATIONAL BUREAU OF STANDARDS REPORTS are usually preliminary or progress accounting documents intended for use within the Government. Before material in the reports is formally published it is subjected to additional evaluation and review. For this reason, the publication, reprinting, reproduction, or open-literature listing of this Report, either in whole or in part, is not authorized unless permission is obtained in writing from the Office of the Director, National Bureau of Standards, Washington 25, D. C. Such permission is not needed, however, by the Government agency for which the Report has been specifically prepared if that agency wishes to reproduce additional copies for its own use.

TABLE OF CONTENTS

Introduction 1

1. Physical Properties of Fluid Hydrogen 1

1.1 P-V-T, Specific Heat, Enthalpy, Entropy, Heat of Vaporization 1

1.2 Thermal Conductivity 7

1.3 Dielectric Constant 16

1.4 Sonic Velocity 16

2. Cryogenic Instrumentation 17

2.1 Forced Vibration Densitometer Study 18

3. Cryogenic Design Principles and Materials Utilization 21

3.1 Propellant Tank Insulation 21

3.2 Properties of Cryogenic Materials 23

3.3 Zero-Gravity Test Container 25

3.4 Zero-Gravity Vent Devices 26

3.5 Safety 27

3.6 Charts of Thermodynamic Properties of Hydrogen 27

3.7 Conclusions 33

Figure 1 - Compressibility Data for Normal Hydrogen 2

Figure 2 - Progress Summary: PVT and C_v Apparatus, 10/20/59 4

Figure 3 - Progress Summary: PVT and C_v Apparatus, 10/20/60

Figure 4 - Sample "Pseudo-Isochore" for Normal Hydrogen 6

Figure 5 - Schematic Diagram of Calorimeter 8

Figure 6 - Schematic Diagram of Thermal Conductivity Apparatus 9

Figure 7 - Schematic Diagram of Thermal Conductivity Cryostat 10

Figure 8 - Pressure Bomb 11

TABLE OF CONTENTS - (Cont'd)

Figure 9 - Gas Handling and Purification Apparatus 12

Figure 10 - Electrical Instrumentation Console 13

Figure 11 - Apparatus for Testing Pressure Transducers 19

Figure 12 - Model of Densitometer 20

Figure 13 - Joule-Thomson Inversion Curve of Hydrogen 32

Appendix I- The Thermal Properties of Gaseous and Liquid Hydrogen Below 60°K 34

INTRODUCTION

Although the work on this program officially started in March, 1960, little effort could be devoted to it until about July 1, because of staffing difficulties. For this reason, the first quarterly progress report was delayed until the present time. This report follows the outline set forth in the statement of work and consists of three main parts:

1. Determination of the Physical Properties of Hydrogen,
2. Cryogenic Instrumentation, and
3. Design Principles and Materials Utilization.

1. Physical Properties of Fluid Hydrogen

1.1 P-V-T, specific heat, enthalpy, entropy, heat of vaporization.
Dr. R. D. Goodwin (Project Leader), D. E. Diller, H. M. Roder, Dr. L. A. Weber, Dr. B. A. Younglove

CEL started work on the tasks in this section on March 1, 1958. R. B. Scott and R. D. Goodwin carried out the early planning of the experimental program. The setting up of the laboratory was done by R. D. Goodwin with help from various assistants, not all of whom are listed above. The immediate effect of NASA support has been to increase the staff from three to five scientists. Although recruiting efforts began early, the two additional scientists could not be obtained until September, 1960. Thus NASA support of this project effectively began only one month ago. In order to convey the entire background of this project, a review from its beginnings will now be presented.

First, we direct attention to a survey of the published data on the thermal properties of fluid hydrogen at low temperatures which is of value as a guide to the areas where more experimental research is needed. Because of its length, this survey which has been extracted from an earlier report, has been placed in an Appendix. It should be noted that the extensive P-V-T data referred to are for normal hydrogen. The extent of coverage is indicated in Figure 1. A more detailed correlation of the P-V-T data for normal hydrogen has been published by Stewart and Johnson[1] of this laboratory. The present investigation

---

[1] R. B. Stewart and V. J. Johnson, Advances in Cryogenic Engineering, Vol. 5, pp. 557-565, 1959

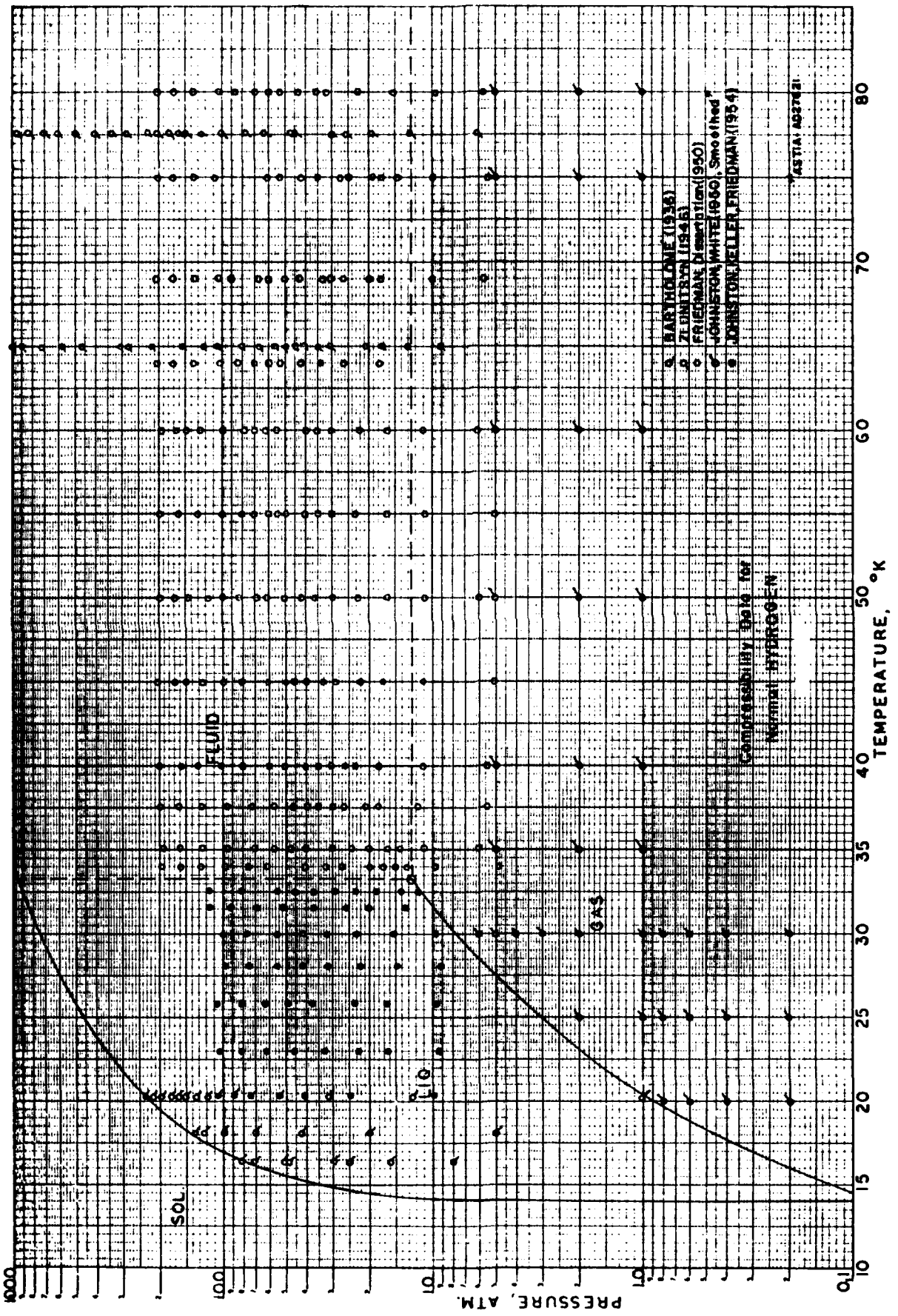

FIGURE 1

is aimed at para-hydrogen, the form that is produced for large-scale cryogenic uses.

The experimental apparatus at CEL consists of two major parts: (1) the P-V-T apparatus and (2) the calorimeter for measuring specific heat at constant volume and the latent heat of vaporization. Of these, the former is completed and is producing data, while the latter is much less far along. The progress as of a year ago and as of now is indicated in Figures 2 and 3, respectively. The calorimeter task has been inactive in the last year. The NASA support will permit resumption of this task and carrying on the construction of apparatus for it simultaneously with the accumulation of P-V-T data.

The experimental tasks are being carried out with what are conceived to be the best available techniques consistent with the time schedule that has been adopted. We can hardly hope to convey in these reports the careful attention to detail that is required in such accurate experimentation and must be content with brief summaries of the principal features.

The P-V-T apparatus consists of a small pressure vessel mounted in a cryostat and equipped with precise means for regulating and measuring its temperature. It connects via a capillary and a pressure-balancing diaphragm cell with an accurate dead-weight rotating-piston pressure gage. Temperatures down to 20°K and pressures up to 5000 psi can be attained and accurately measured. Results of one "pseudo-isochore" for normal hydrogen are shown in Figure 4. The resulting compressibility factors agree, on the average, within 0.1% with the best published values. Following this experiment, which was for the purpose of testing the apparatus, sixteen pseudo-isochores of para-hydrogen have been obtained at molal volumes from 28 to 40 cm^3. Further measurements will be made at both higher and lower densities. In looking ahead to the problem of how to correlate a wide range of P-V-T data, Goodwin has developed an approximate empirical equation of state.[2]

---

[2] R. D. Goodwin, Advances in Cryogenic Engineering, Vol. 6, Paper G-4, 1960 (in press)

PROGRESS SUMMARY: PVT and C_v APPARATUS

10/20/59

APPARATUS	WORK PHASE 1 Designed	2 Acquired	3 Installed	4 Tested	5 Calibrated	REMARKS
I. Compressibility Apparatus						
1 Cryostat	X	X	X		-	Vacuum tested, room temp.
2 Sample-holding pipet, volume	X	X	X		1/3	Must calibrate with gas
3 Cryostat electric wiring	X	X	X	1/2	-	Tested, room temp.
4 Refrigerant transfer systems and cool-down controls	X	X	(X)		-	Transport dewar pressure control?
5 Dewar pumps, valve manifolds, gages	X	X	X	X	-	--
6 Pure sample cylinders and stock	X	X	(X)		-	To be analyzed; cylinder valve manifolds
7 Sample preparation systems, purification, compression, o-p conversion	X	X	9/10		-	Regeneration details
8 Sample distribution, measuring system, HP valve manifolds	X	X	X			Must calibrate volumes
9 O-P gas analysis system	-	X				--
10 Precision gasometer system, manifolds, volumes, thermostat, manometer, burette	X	2/3	2/3		1/3	Manometer on order
11 Precision pressure measuring system, includes dead weight gage	X	X	9/10	(X)		Tested without gas; NPD cleaning problem
12 Precision temp. measuring systems, incl. thermometer. potentiometers, etc.	X	X	9/10			Awaits platinum thermom. calibration
13 Pipet temperature controls	X	X	X		-	--
II. Specific Heat Apparatus (Additional)						
1 Cryostat with adiabatic shields	X	X			-	--
2 Sample-holding calorimeter	(X)	(X)				S.S. spheres - require special study
3 Cryostat electric wiring	X				-	--
4 Precision resistance thermom.	X					--
5 Precision shield temperature controls, amplifiers, controllers, recorders, power supply	(X)	(X)	(X)		-	Two systems on hand. More" May want L.N. "C.A.T." controllers
6 Precision calorimetric heat control and measuring instruments	X	X	X			--

FIGURE 2

PROGRESS SUMMARY: PVT and C_v APPARATUS

10/20/60

APPARATUS	WORK PHASE 1 Designed	2 Acquired	3 Installed	4 Tested	5 Calibrated	REMARKS
I. Compressibility Apparatus						
1 Cryostat	X	X	X	X	-	In operation
2 Sample-holding pipet, volume	X	X	X	X	X	In operation
3 Cryostat electric wiring	X	X	X	X	-	In operation
4 Refrigerant transfer systems and cool-down controls	X	X	X	X	-	In operation
5 Dewar pumps, valve manifolds, gages	X	X	X	X	-	In operation
6 Pure sample cylinders and stock	X	X	X	X	-	In operation
7 Sample preparation systems, purification, compression, o-p conversion	X	X	X	X	-	In operation
8 Sample distribution, measuring system, HP valve manifolds	X	X	X	X	-	In operation
9 O-P gas analysis system	-	X	X	X		In operation
10 Precision gasometer system, manifolds, volumes, thermostat, manometer, burette	X	X	X	X	X	In operation
11 Precision pressure measuring system, includes dead weight gage	X	X	X	X		In operation
12 Precision temp. measuring systems, incl. thermometer, potentiometers, etc.	X	X	X	X	X	In operation
13 Pipet temperature controls	X	X	X	X	-	In operation
II. Specific Heat Apparatus (Additional)						
1 Cryostat with adiabatic shields	X	X	1/2		-	--
2 Sample-holding calorimeter	(X)	(X)				S.S. spheres - require special study
3 Cryostat electric wiring	X				-	--
4 Precision resistance thermom.	X	X				--
5 Precision shield temperature controls, amplifiers, controllers, recorders, power supply.	(X)	(X)	(X)		-	Two systems on hand. More? May want L. N. "C. A. T." controllers.
6 Precision calorimetric heat control and measuring instruments	X	X	X			--

FIGURE 3

FIGURE 4

SP VOL CC PER GM MOL	DENSITY GM MOL PER CC	PRESSURE ATM	TEMP. DEG. K	COMP FACTOR PV/RT	PROJECT RUN NO. POINT NO.
2664825052	3752591649	2232575153	4000000052	1812588351	8153100101
3044274852	328454649	3086900652	2800000052	4090089650	8153100201
3045950252	3283047849	4535708952	3000000052	5612173450	8153100202
3047567552	3281305549	5973785652	3200000052	6933257950	8153100203
3049155652	3279596549	7408539152	3400000052	8096878350	8153100204
3050761152	3277870649	8844332652	3600000052	9133876350	8153100205
3053764052	3274647349	1169687653	4000000052	1088252751	8153100206
3057353552	3270802749	1518837853	4500000052	1257560551	8153100207
3060739752	3267184149	1862131153	5000000052	1389156051	8153100208
3063857252	3263859749	2200327753	5500000052	1493748851	8153100209
3066915052	3260605549	2533102953	6000000052	1577929951	8153100210
3069825552	3257514149	2860784753	6500000052	1646530951	8153100211

Comparison of compressibility factors for Run #2

Source	Comp. factor Source	% Deviation Source-ours / source
Friedman Report 3282	.40926	.0611%
	.56159	.0659
	.69452	.171
Johnston et al	.9136*	.0219
Trans. ASME	1.0902	.174
	1.259*	.079
	1.3928	.258

*Non-linear interpolation of source required.

The above data resulted from a processing of all the experimental data by an automatic computer. The decimal point is located at the left of the printed numbers, and the last two digits minus 50 give the power of 10. Thus 1234567852 means 0.12345678×10^{2}.

A preliminary design of the calorimetric apparatus was made at an early stage. This was desirable because it was intended to use some of the same temperature control and measurement equipment and sample-handling apparatus for both the P-V-T and calorimetric experiments. Thus some degree of coordination in the early planning was required. Steel hemispheres for the pressure vessel were acquired, but construction of the calorimeter was then set aside in order to progress with the P-V-T apparatus. In the past month, the calorimeter has again been taken up and will now be completed. The pressure vessel is being assembled, and principles of thermal shielding are being examined. An early schematic diagram of the calorimeter is shown in Figure 5 and will serve to suggest the general principles to be used.

1.2 Thermal Conductivity

W. J. Hall and R. L. Powell

This task also was initiated in March, 1958. A guarded flat-plate configuration was adopted for the experimental cell. As in Section 1.1, temperatures down to 20°K and pressures up to 5000 psi can be attained. Figures 6 and 7 show the apparatus schematically, while Figures 8, 9, and 10 are photographs of the pressure bomb, the gas handling and purification apparatus, and the electrical instrumentation console, respectively.

The thermal conductivity, K, is defined by the Fourier equation:

$$W = - KA \frac{dT}{dX}$$

when W is the heat flow, A is the cross-sectional area, and dT/dX is the temperature gradient in the direction of heat flow. Since the measurements will be made at equilibrium, and since the property being measured is macroscopic instead of microscopic, the thermal conductivity is approximated by the equation:

$$K = \frac{W\ (\Delta X)}{A\ (\Delta T)}$$

where W is now the power put into the hot plate (See Figure 6). This is determined by measuring the current flowing in the hot plate heater and the voltage impressed upon it. The cross sectional area, A, and the distance between the hot and cold plates, ΔX, are determined at room temperature and corrected for temperature and pressure.

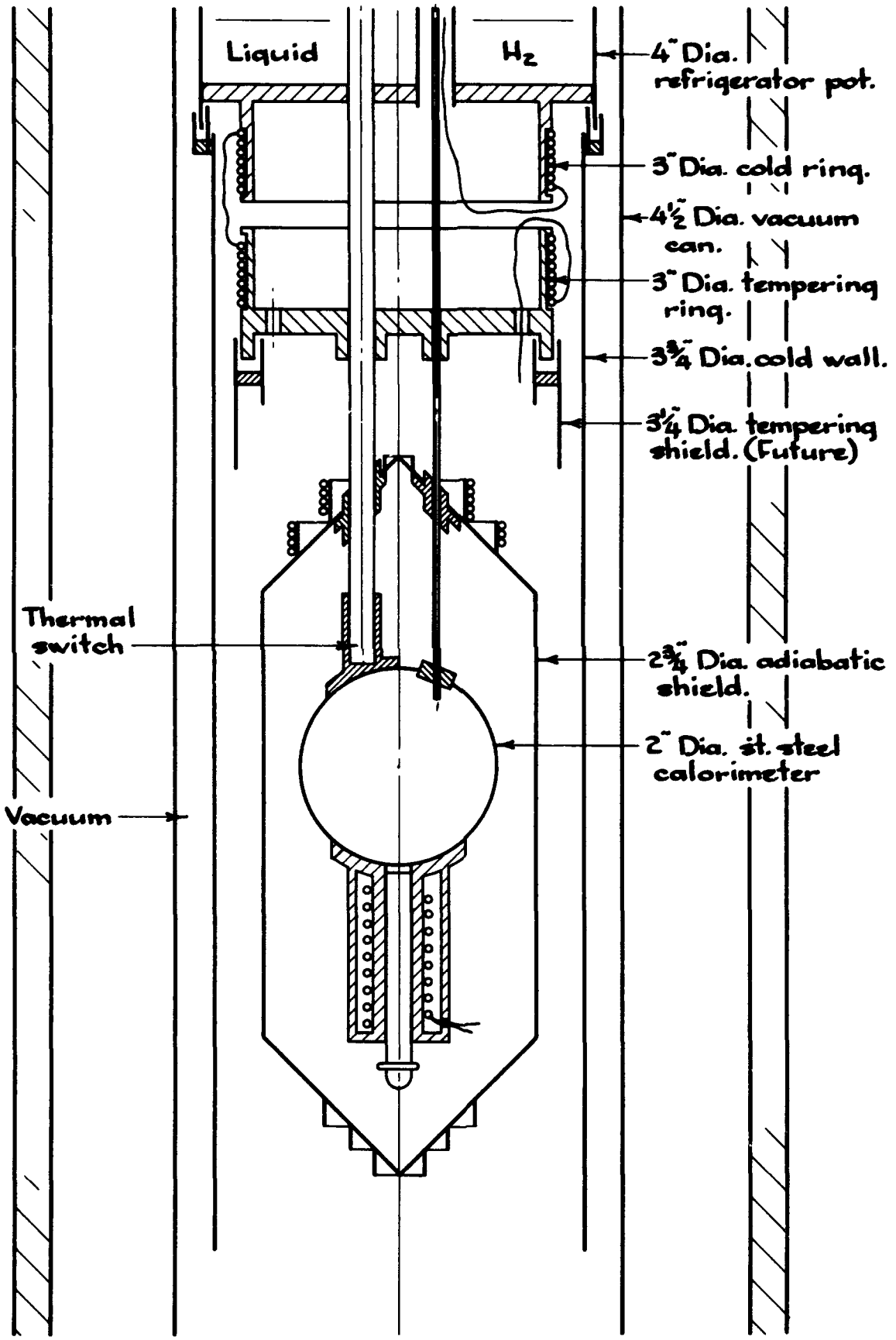

Fig. 5

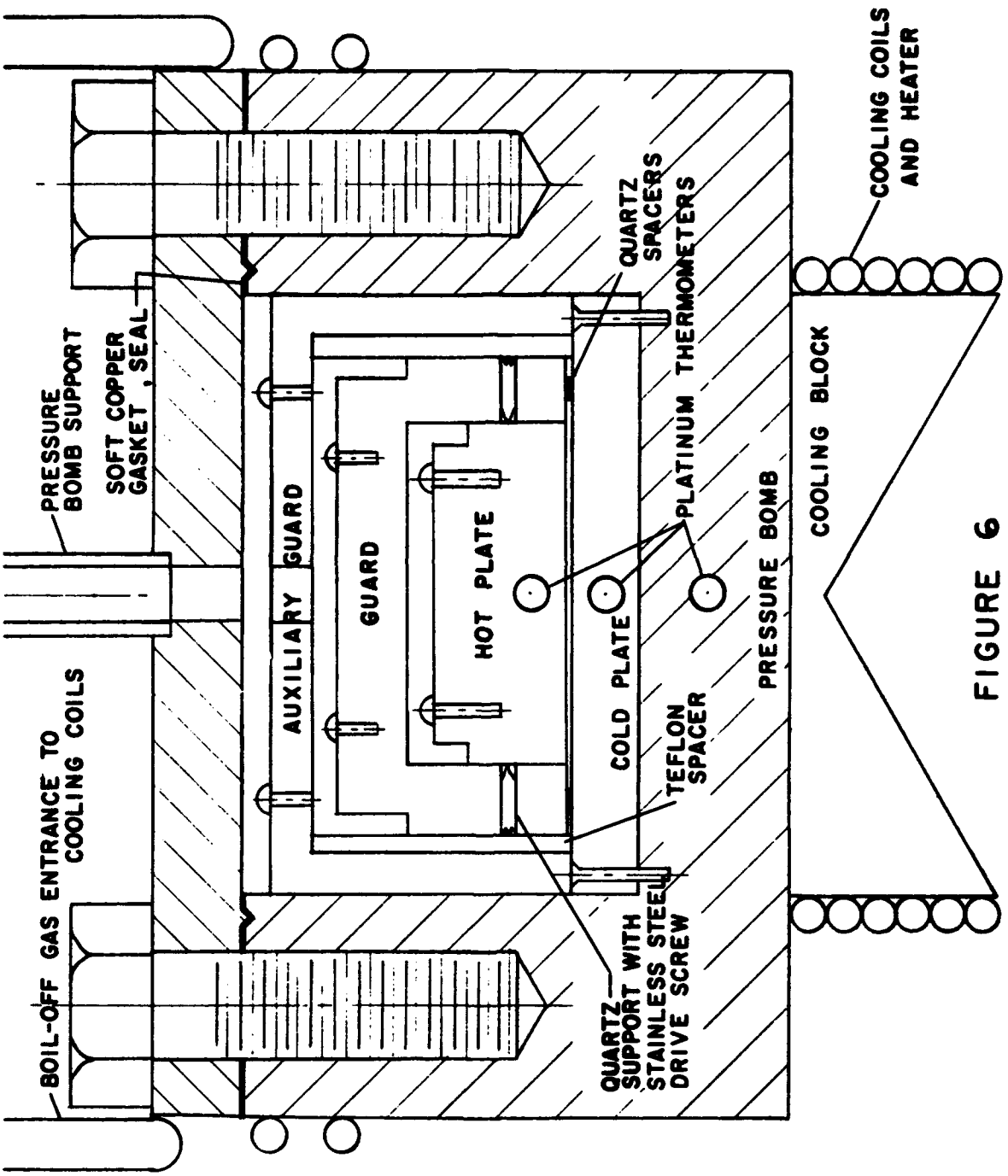

FIGURE 6

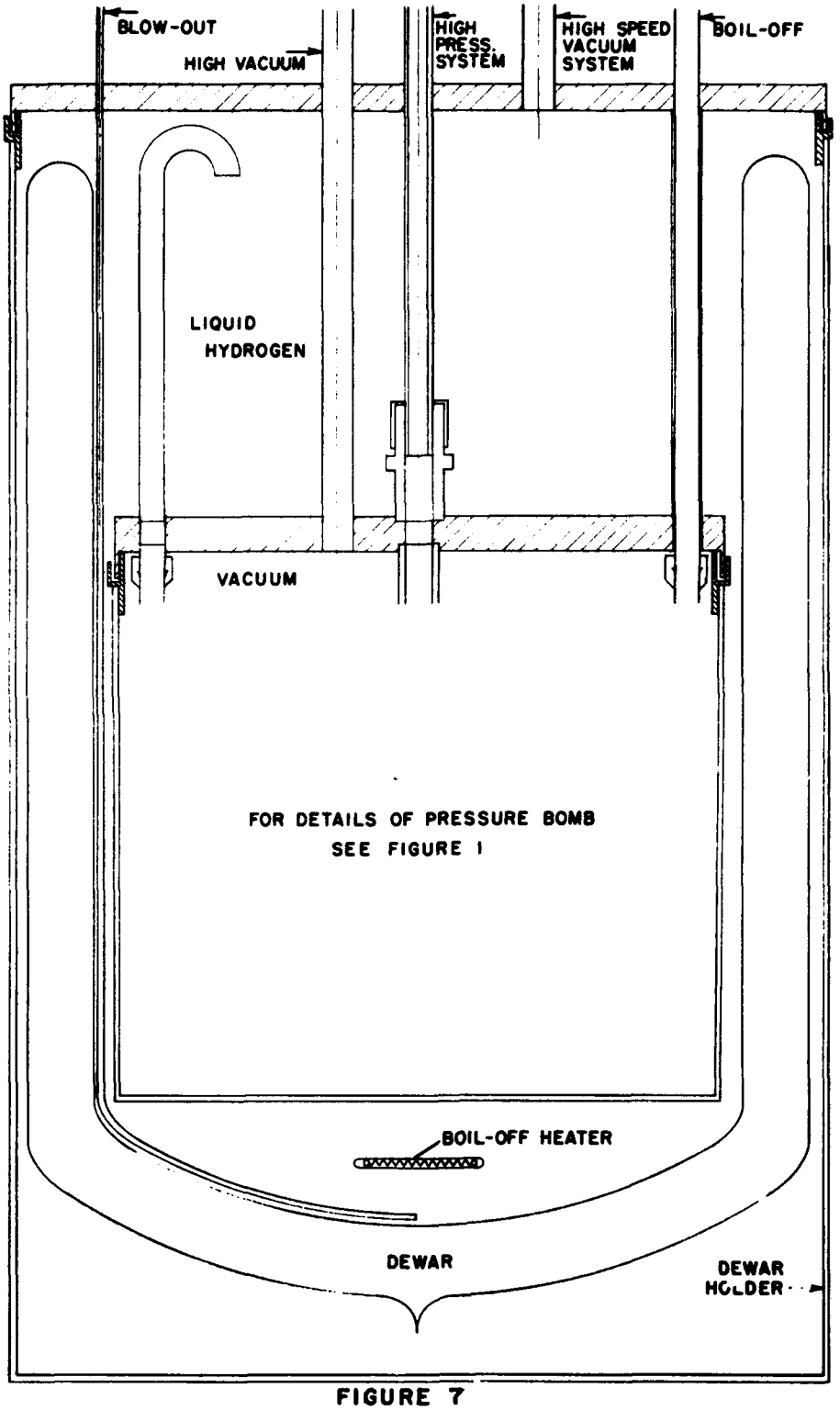

FIGURE 7

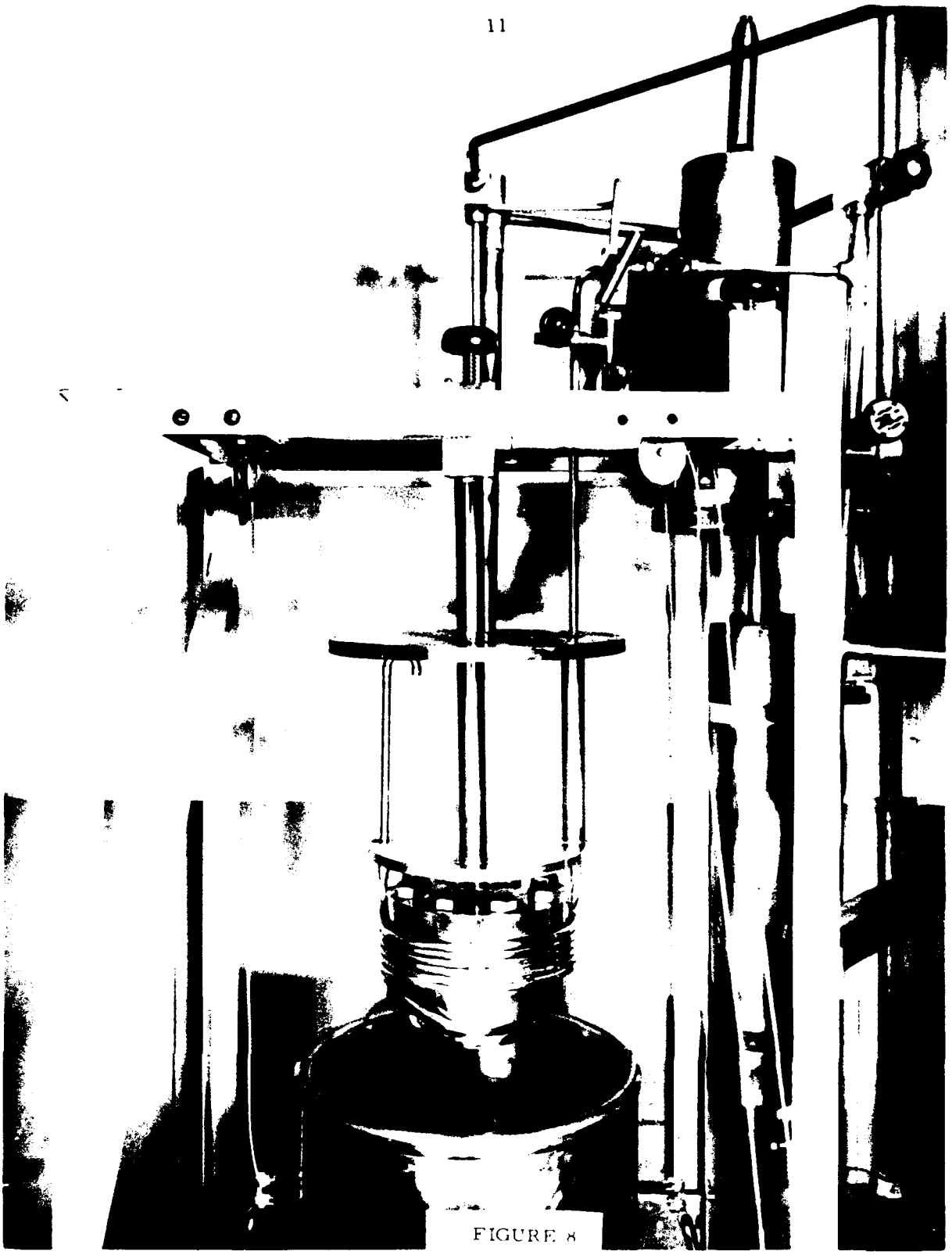

FIGURE 8

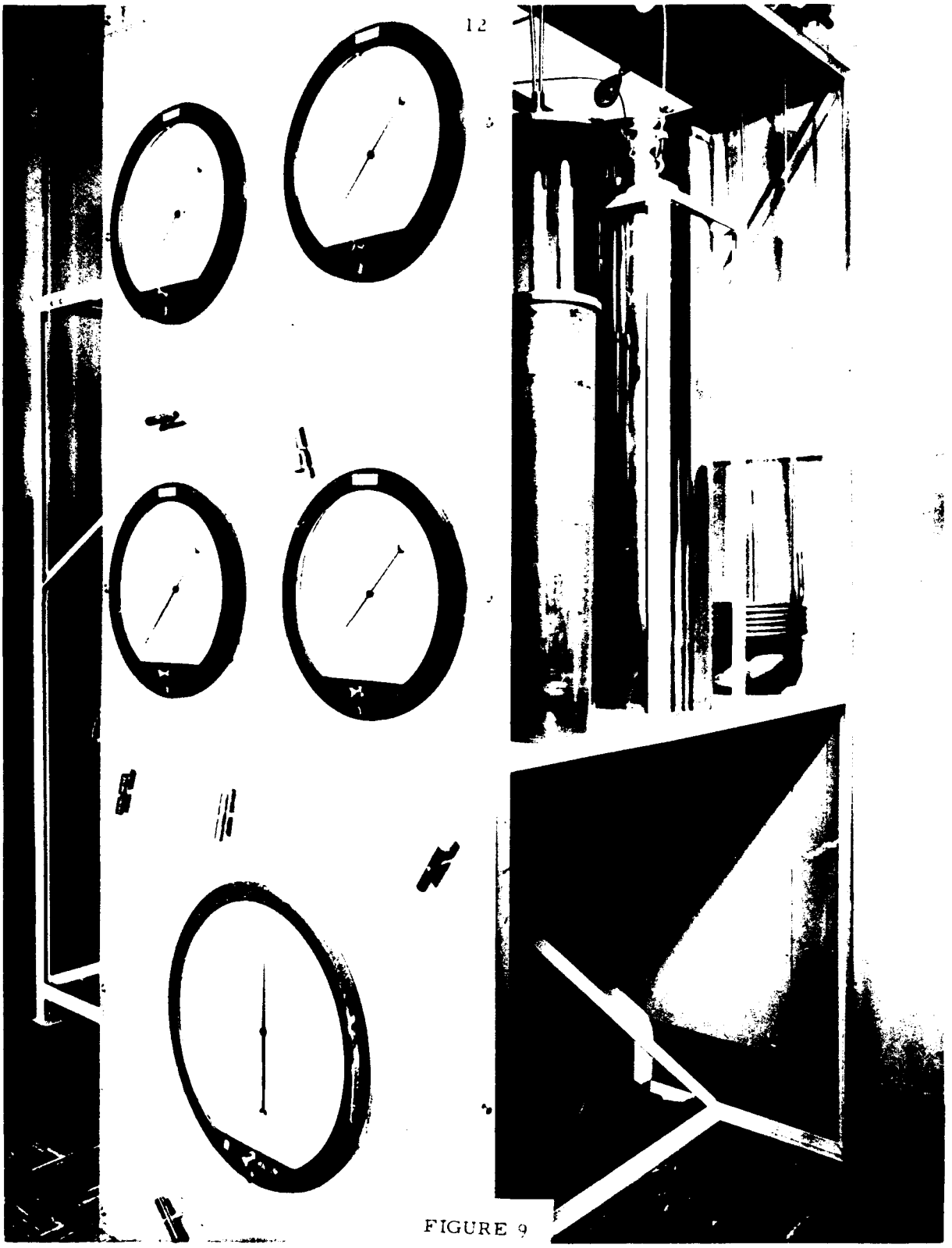

FIGURE 9

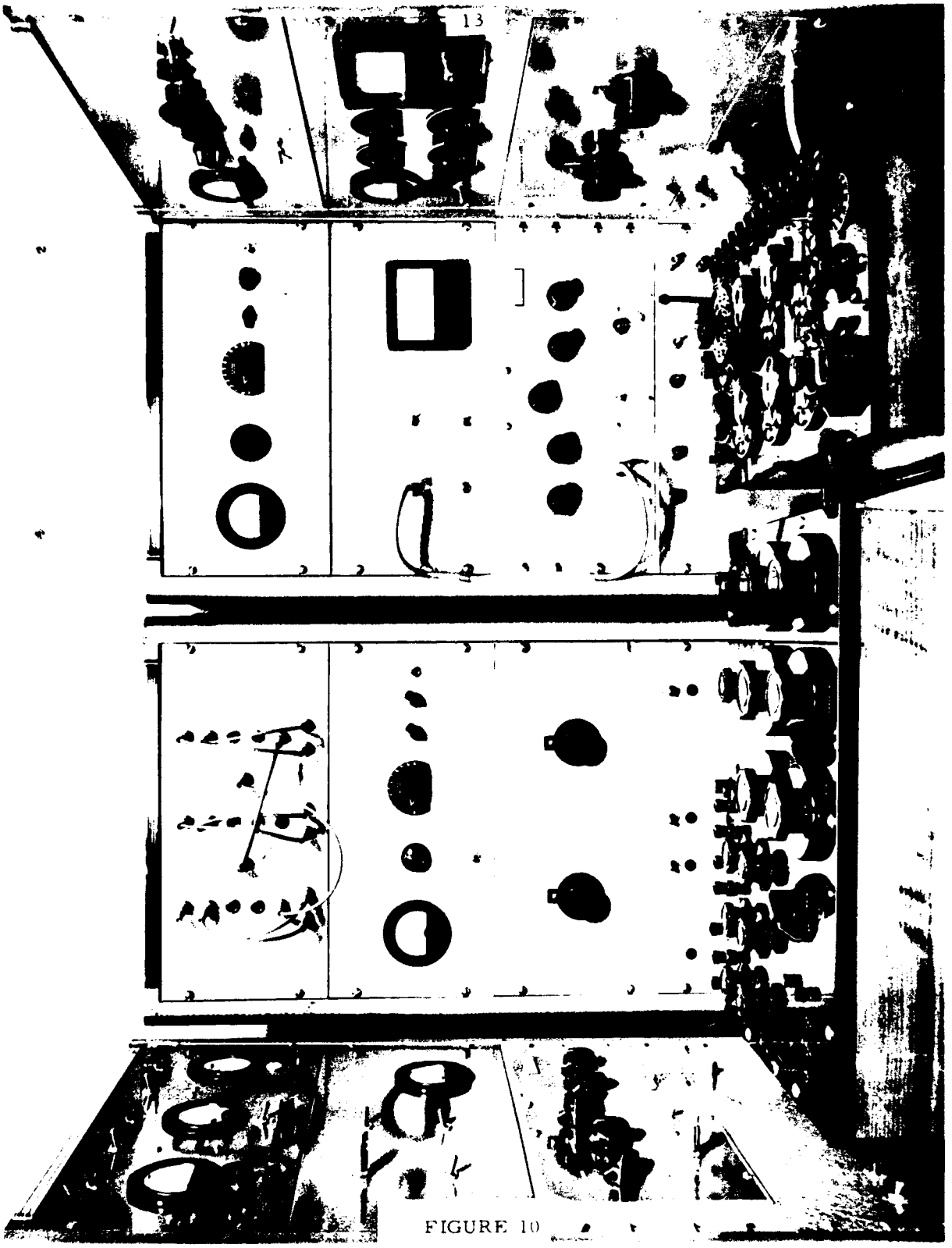

FIGURE 10

The temperature difference between the hot plate and the cold plate, ΔT, is measured both by platinum resistance thermometers and by difference thermocouples.

Heat flow from the hot plate will be nearly linear into the cold plate since the hot plate is surrounded by a guard which will be held at the same temperature as the hot plate to within 0.001°K by a thermopile composed of eight difference thermocouples. The auxiliary guard is needed to prevent excessive cooling of the guard by cold gas flowing into the pressure cell from above.

The hot plate is supported in three places by quartz spacers forced into it by stainless steel screws. After the hot plate and guard were fastened together they were machined smooth on the bottom. Fused quartz spacers placed under the guard support both the guard and the hot plate above the cold plate. Several values of ΔX, e.g. 0.25, 0.50, 1.00 mm. are available.

The temperature of the hot plate and cold plate are measured by platinum thermometers imbedded in them and open to the pressure in the cell. Since the difference in temperature is more easily stabilized from thermocouple output, thermocouples have been installed in parallel with the platinum thermometers. The absolute temperature is measured by a sealed platinum thermometer imbedded in the wall of the pressure cell.

It is possible, in fact, necessary, to determine the pressure coefficients of resistance for the unsealed platinum thermometers and the thermocouples used. This can be accomplished with this arrangement since the cold plate platinum thermometer and the calibrated, sealed platinum thermometer in the cell wall are well-connected thermally.

To keep the measuring components as isothermal as possible, they have been fabricated from electrolytic tough pitch (99.9 per cent pure) copper. It was necessary to make the pressure cell of beryllium copper to contain the pressure even though its thermal conductivity is undesirably low. To improve the heat flow pattern, a cooling block is attached to the bottom of the pressure cell (See Figure 6). Heaters and difference thermocouples were put in various places on the pressure cell to make it as isothermal as possible.

The measuring components and associated pressure container are supported from above by a stainless steel tube through which the electrical wiring enters the measuring cell. This tube thermally isolates the pressure cell from the boiling cryogen. By controlling the amount of boil-off gas passed through the cooling coils and the power input to the external heaters, the measuring cell can be raised to desired temperatures above the boiling point of the cryogen. The large heat capacity of the cell facilitates temperature stabilization.

The foregoing apparatus was nearly all completed prior to initiation of NASA support. During the period covered by this report, calibration of the platinum resistance thermometers within the gas space of the cryostat has proceeded smoothly and regularly. Measurements have been made at five well-separated temperatures and at pressures of 0.1, 1, 10, 50, 100 and 250 atmospheres. As expected, the resistances of the thermometers vary linearly with temperature, so that calibration and interpolation calculations are both simple and accurate. The pressure changes during an experimental run are undetectable for the lower pressures and only about one part in a thousand for the highest pressures. The temperature drifts of the cold and hot plates within the cryostat are held to about 1 to 3 x 10^{-4}°K for each run. A refinement in measuring techniques has pushed down the uncertainties in measurement of temperature differences to about the same level. A servo-control for the power supply to the main block heater has brought about both a more rapid approach to steady state conditions and also smaller cyclic variations in the block temperature.

The calibration runs have had the special additional benefit of revealing fine details of the temperature distributions within the system. It was found recently that there were gradients of up to 0.01°K between the cold plate and the block and that these gradients were pressure dependent. The expected limit of accuracy for the system as a whole is also about 0.01°K. However, the gradients mentioned would have no effect, in the first approximation, on actual thermal conductivity readings. Nevertheless, the system is being changed slightly in order to reduce minor fluctuations in the later measurements.

The gradients were caused by the cooling of the outer guard and the subsequent cooling of the inner guard, hot plate, and cold plate. The cooling of the outer guard was caused by conduction up the copper wires and by gas conduction to the upper plate of the large pressure block. The gradients observed were pressure dependent because the gas conduction from the outer guard to the inner parts was itself

pressure dependent. The new additions to the cryostat are: (1) a heater on the outer guard to balance the heat conduction up the wires; and (2) a heater on the top plate of the block to bring it into thermal equilibrium with the main part of the block. The necessary auxiliary power supplies and contrcllers are being placed on the instrument panels.

Following completion of the thermometer calibrations, a brief series of measurements will be made on air at low pressures in connection with another project. The apparatus will then be devoted to making the more extensive high-pressure measurements on para-hydrogen.

1.3 Dielectric Constant

Experimental measurements of dielectric constant are being deferred for the present for the following reasons:

a. Examination of the published data for normal hydrogen shows that the Clausius-Mosotti equation fits the best data within about 1% in $(\epsilon - 1)$ over a very great range of conditions from low pressure gas at ambient temperature to saturated liquid. This indicates that only a few experimental measurements will need to be made in order to establish the pattern of the deviation (if any) from the equation. Interpolation throughout the P-T-ρ region of interest can then be made using the equation rather than by direct measurement. Since the experiment will be a relatively simple one, it does not have to be started at once. Also, the correlation of the results would have to wait anyway on the availability of accurate data from the P-V-T project.

b. At a later date, it may be possible to use a pressure cell, cryostat, and gas handling equipment developed for one of the other tasks, such as the one on thermal conductivity, and thus avoid duplicating this expensive equipment.

1.4 Sonic Velocity

We have attempted vigorously to recruit a man with experience in ultrasonics for this task, but have not been successful as yet. Some good prospects were lost because the recent federal pay raise and liberalization of Civil Service hiring procedures for top-quality Ph. D. 's came a little too late relative to the period, February-May, when most

recruiting is accomplished. Recruiting efforts will continue, of course, with the aim of providing a top-quality project leader. Consultative services in ultrasonics are already available within NBS.

2. Cryogenic Instrumentation

J. Macinko, P. Smelser, R. C. Muhlenhaupt, C. E. Miller, R. B. Jacobs

The first phase of the Cryogenic Instrumentation project is the determination of the status of instrumentation in the areas of pressure, temperature, liquid level and flow rate measurement. A survey of technical publications revealed that very little had been published with regard to response and performance characteristics; the bulk of the literature was descriptive in nature but in many cases the theory of operation was also covered.

Letters of inquiry were sent to industries and laboratories known to be working in cryogenics requesting information on the use of instruments in their facilities. The answers received were helpful in providing direction for future test programs. However, many inquiries remain unanswered and many answers were uninformative; the overall result was disappointing.

Several reports of the results of test and evaluation programs were also studied. Some of these reports are excellent in content and organization. This study indicates that broader coverage of the field is definitely required. In addition, testing in the cryogenic region has been very limited. Manufacturer's literature and performance specification sheets provide additional information, but in most cases the manufacturers have not provided performance characteristics in temperature and pressure regions of importance to the cryogenic industry.

Due to the above factors, the first phase of the instrumentation survey contains very little evaluation based on controlled tests or user application. However, a compilation of the various methods of measurement of the four parameters under study, the physical principles involved, and a partial list of manufacturers of the instruments under investigation may be of immediate value to engineers, scientists and technicians engaged in cryogenics. This compilation is nearing completion and has been set up using an orderly index which permits additions under all classifications and subheadings. Instruments have

been evaluated wherever experience or data permitted. Additions and revisions will be made as test results and manufacturers' literature are received.

A test program is planned for all phases of the study and will be entered into progressively. An apparatus has been designed and built for testing pressure transducers (Figure 11) and will soon be ready for its initial cooldown and performance evaluation. An idea for a densitometer is being studied and a model has been built and will be tested within the next month (Figure 12). Several ideas have been investigated for determining response time of temperature sensors and final plans of a test apparatus will be drawn up shortly. No additional test plans have been formulated to date, but additional testing will be planned as soon as our studies indicate which parameters should be measured, the conditions under which measurements should be made, and the degree of accuracy required in testing.

2.1 Forced Vibration Densitometer Study

An experimental program is being conducted to determine the feasibility of using a vibrational system as a means of determining fluid densities. The underlying idea is that the mass of a vibrating system is a primary factor in determining the dynamic characteristics of the system. If certain characteristics of the system are appreciably affected by the density of the fluid flowing through the system, a properly instrumented system will provide a means for measuring density.

The choice of the system has depended on many things, among which, and perhaps most important, is the reliability and accuracy of associated mechanical and electronic instruments.

Figure 12 illustrates the system that is presently being investigated. The flow passage is supported by bellows with an effective transverse spring constant k_B. The passage is being driven with a scotch yoke mechanism which has been designed to transmit a sinusoidal motion with an amplitude X_o sufficiently large to influence the fluid. The motion of the drive mechanism is transmitted through a force gage to the passage. A force transducer with an extremely high spring constant has been selected. By making the spring constant large enough, we can make the assumption that

$$X_{(t)} = X_{(f)}$$

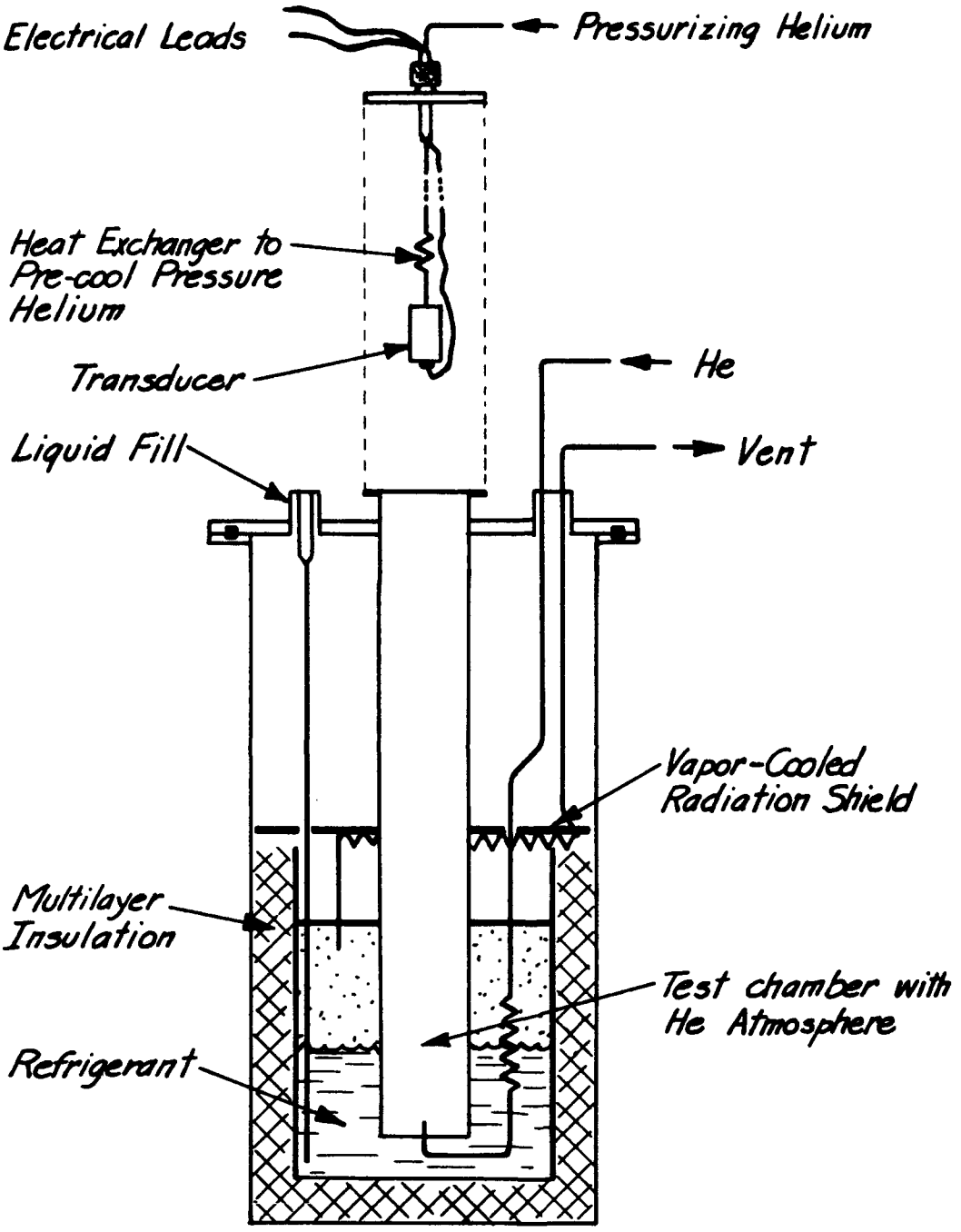

FIGURE 11.
Cryostat for low temperature testing of pressure transducers.

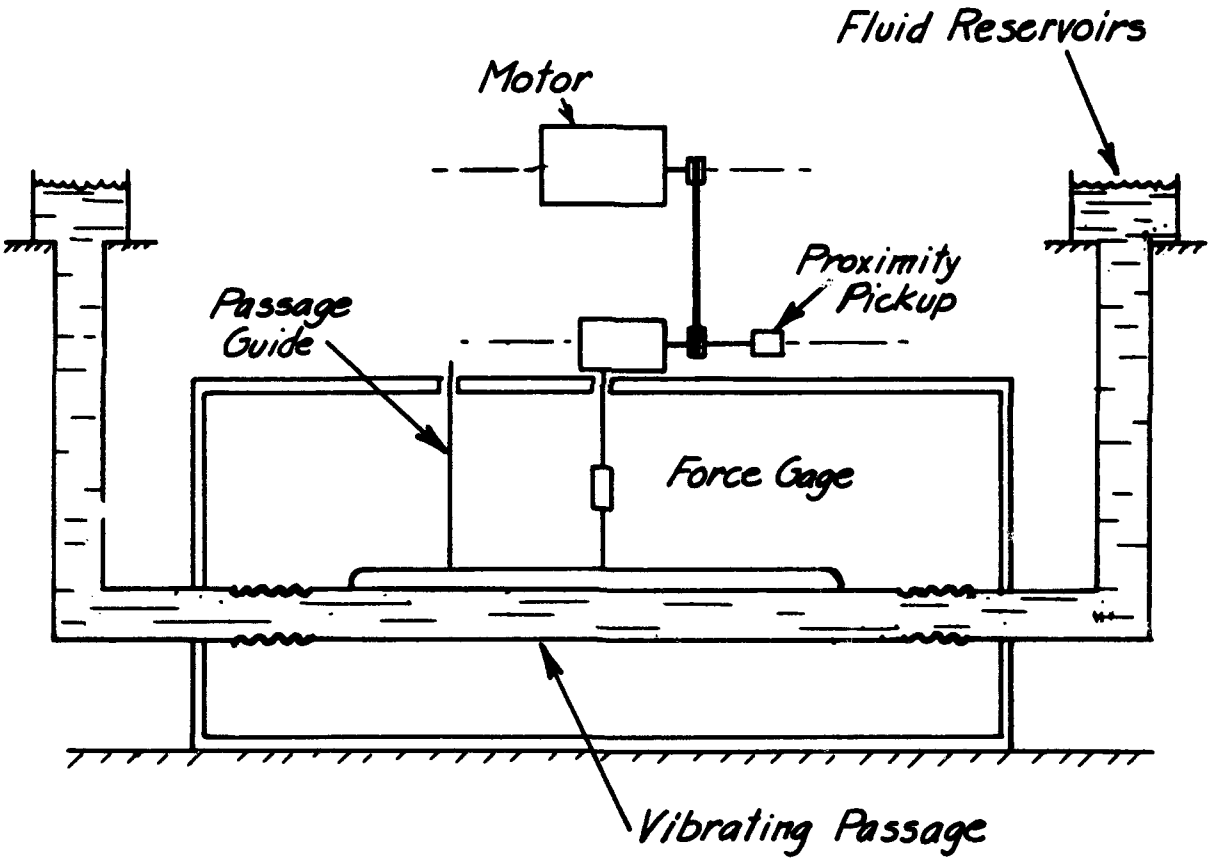

FIGURE 12.
Densitometer test apparatus.

where $X_{(t)}$ is the transverse motion of the passage and $X_{(f)}$ the forcing function. Writing the equation of motion of the system we have

$$M\ddot{X} + C\dot{X} + K_B X = F$$

where M is the total mass of the system ($M = m + \rho V$), and m is the effective mass of all the vibrating mass except the fluid, V is the volume of the passage, and ρ the density of the fluid. Some damping is inherently involved in this type of system and is shown as $C\dot{X}$.

It can be shown from the equation of motion that by measuring the force being transmitted to the passage at the point of maximum acceleration that the density parameter can be attained and is related to the force by the following equation

$$\rho = A + BF$$

where A and B are constants that can be determined experimentally.

3. Cryogenic Design Principles and Materials Utilization

D. B. Chelton and B. W. Birmingham

The statement of work calls for a survey to be initiated by NBS in the broad area of cryogenic design principles and materials utilization to provide support for the Centaur and Rover program. It has been difficult to know exactly how such a task should be conducted. To get things started, contact has been made with Convair Astronautics regarding Project Centaur and the Los Alamos Scientific Laboratory regarding Project Rover. Two visits were made to Convair Astronautics and several telephone discussions have taken place. In addition, personnel from Convair Astronautics have visited CEL on at least two separate occasions. Telephone conversations have also taken place with LASL personnel, and members of LASL divisions N, J, and CMF visited CEL to discuss cryogenic engineering problems on Rover and determine what research was currently underway at CEL. Some progress has been made in this manner both in learning about problems and becoming acquainted with project personnel.

A detailed description of some of the technical problems that have been considered on Project Centaur follows:

3.1 Propellant Tank Insulation

The insulation of the Centaur propellant tank has been studied and several problems encountered.

Improper application of the insulation on the forward bulkhead of the fuel tank can condense a sizable quantity of air. This can result in several undesirable conditions: (a) The solid and/or liquid air can add considerable dead weight to the vehicle. (b) The solid air can freeze the side insulation panels in place so they cannot be jettisoned when required. (c) The condensation process can add considerably to the anticipated fuel evaporation rate by increasing the "apparent" thermal conductivity of the insulation.

The method of application of pre-formed insulation does not completely cover the tank to assure sufficient vapor barrier to prevent condensation of air. Also certain areas, dictated by geometry, may prevent application of pre-formed insulation. A suitable bonding agent may also represent a formidable problem area.

The spray foam method of applying insulation has been developed by Convair Astronautics and other investigators to a point where serious consideration should be given to such application on the forward bulkhead. This technique will form a much better vapor barrier especially over the parts having difficult geometrical configurations. In the past, great difficulty has been experienced with foams breaking away from the surface and cracking when thermal cycled. However, it appears, from the limited experimental data available that Convair Astronautics may have solved the adhesion and cracking problems with their present spraying technique. These data are available on small tanks only, and initial tests showed good adhesion for a single cool-down. However, thermal cycling experiments, done later at the suggestion of CEL, induced failures. Proper surface cleaning techniques recommended by CEL resulted in greater success. Thus, once again it is shown that fabrication control techniques are essential when applying these foams.

CEL has available a company to spray foam samples (in Boulder, Colorado) if additional data are required. A limited number of tests could be conducted if additional information is needed to back up the work being done at Convair. It is unfortunate that Convair did not know of research that has been carried out by NBS, Beechcraft Research and Development, and Armour Research Foundation. The latter organization has been working for a number of years to perfect such insulation methods.

Although the insulation program at Convair Astronautics is meeting with a good degree of success, a more fundamental approach to the problem would seem advisable. The accelerated time schedule present in their program is well recognized. However, a parallel program could be established to more fully understand the pertinent considerations of the application. For instance, it has been found by previous investigators that slight variations in foam composition, surface finish and preparation, method of application, spray timing sequences, etc., materially influence the results. It is therefore conceivable that a success on one tank would not necessarily insure success on all tanks unless a high degree control is exercised in both application and foam composition. Since the important factors of foam composition are not fully understood, the aforementioned quality control would seem difficult.

3.2 Properties of Cryogenic Materials

General assistance has been given to various groups within the Centaur Project on properties of cryogenic materials -- fluids, structural materials and insulations. Thus far, the assistance has, in general, been acquainting the personnel with properties that already exist in the literature. The Cryogenic Data Book, WADC 59-8 prepared by the NBS is in general use.

a. Fluid Properties

In addition to acquainting personnel with existing data from literature, several problems were studied in connection with the properties of hydrogen in its various ortho-para modifications. An example is the study of several existing temperature-entropy diagrams for hydrogen to determine which is the most appropriate. By basic thermodynamic reasoning, it was possible to disprove the validity of data in certain areas of an often used diagram. Information was also supplied on the gas-liquid phase equilibrium for the system helium - hydrogen. (See Section 3.6, Thermodynamic Charts for Hydrogen.)

Much information is lacking in the low temperature compressed fluid region for hydrogen. These properties are presently being investigated at CEL and will be made available as soon as possible.

b. Material Properties

It is conceivable that certain mechanical, transport and expansivity properties of structural materials applicable to the Centaur Project have not yet been determined. The test facilities at CEL may

be useful in assisting the Convair group in such determinations. However, the present heavy commitments of the CEL mechanical properties project will undoubtedly limit extensive testing in this area. The assistance of CEL staff has already been used by Convair in the establishment of such a testing facility. It is our understanding that this facility is quite active and producing useful results.

c. Bearings

A proposed centrifugal zero-gravity vent device requires bearings which operate surrounded by low-temperature gas phase fuel since liquid cooling cannot be assured. Conventional lubrication is, of course, impossible. A high degree of reliability is essential. Several types of bearings may be practical for such application. Three such bearing types are being explored on other programs at CEL. Gas lubricated and magnetic bearings are presently in the early stage of development. Their development cannot be assured in time to be of use to the present Centaur Project, but may be applicable in later phases.

A test program to evaluate ball bearing materials at cryogenic temperatures has been underway for several years at CEL. However, the program thus far has mainly investigated bearings submerged in cryogenic liquids. To determine the feasibility of using ball bearings operating in cryogenic gases (particularly hydrogen) for the centrifugal vent devices, preliminary experiments were performed in a CEL bearing tester. As a first attempt, the most promising bearing (determined from experiments with the bearings submerged in liquid), was operated in a cold nitrogen (100°K) gas environment. These bearings were constructed of 440 C stainless steel balls and races with Fulon A (reinforced polytetrafluoroethylene resin which contains a highly inert, inorganic silicate base filler) separators. Although the tests were not conclusive since only two such bearings were operated, 10 hours of operation were obtained at 100°K under an essentially no-load condition. At the end of this period there was no noticeable increase in operating torque. On close inspection, the bearings were seen to be slightly roughened. However, it was concluded that the operation of ball bearings in a cold gas environment may be possible.

If it is considered advisable, future tests can be made. In such event, several preliminary "run-in" phases are planned that should greatly increase the bearings' useful life. Convair has been made aware of CEL willingness to perform these future tests. Since

the bearing apparatus is part of another project, the tests would have to be coordinated with the existing program, however, no particular delays are foreseen.

d. Adhesives

The use of epoxy resins for cryogenic applications is discussed elsewhere in the report. Their application at CEL, however, has provided sufficient knowledge to include their use in many instances. An example is the observation windows for the zero-gravity test container.

3.3 Zero-Gravity Test Container

Several discussions were held both at Convair Astronautics and in Boulder concerning the test container for the study of fluid behavior in or near zero-gravity. Other than general cryogenic design principles, assistance was given in two particular areas -- optics and seals.

Design criteria for the successful design of observation windows was established by the Bureau. The success of a window was determined by good structural integrity and by the ability to maintain glass temperatures above the dew point. The basic difference between the present design and other observation windows used elsewhere is reflected in the need for having a support tube between the two windows. Heretofore, it was general practice at Convair to have a helium purge on the warmer window to prevent accumulation of frost. For the present application it was considered impractical to have such a purge. Actual calculations necessary to insure a proper design necessitated several assumptions. To substantiate the design and the assumptions made, laboratory tests were conducted at CEL. Three successful methods of obtaining an observation window were developed. The arrangement most applicable for the subject test container consisted of tapered pyrex glass windows sealed to the metal support tube with epoxy resin. A thin application of Armstrong A-4 epoxy with Activator E was found to work best. The configuration used resulted in a glass temperature only a few degrees below the environment.

Cryogenic seals developed at this laboratory were directly applicable to the test container. However, because of the advanced stage of the design, it seemed impractical to make use of these developments. The seals used are not suitable for an absolute seal,

but should be suitable to prevent major leakage of hydrogen gas. Although it should be noted that one hydrogen fire developed on a Point Loma test stand because of a faulty seal.

The low refractive index of liquid hydrogen calls for rather specialized illumination and photographic systems. For saturated liquid hydrogen at one atmosphere, the refractive index is 1.1097 for a wavelength of 0.5790 μ. This gives a large forward scattering of light. The difficulties of right angle illumination (with respect to the camera) may be illustrated from the fact that the scattering of light from a hydrogen bubble is 10,000 times greater at 2° from the direction of illumination than at 90°.

Direct or right angle illumination of certain test containers, however, often results in satisfactory photographs. It is felt that this is due primarily to multiple reflections from the highly reflective tank walls. Under certain conditions (dull tank walls) the events within a vessel may be obscured by using such illumination.

3.4 Zero-Gravity Vent Devices

Vent devices for the fuel tank under conditions of zero-gravity have been considered in some detail. A great number of venting methods exist, although these may basically be classified as centrifugal and thermodynamic. Convair is designing and fabricating a centrifugal device and is also considering thermodynamic devices. In addition to this approach, an outside contractor will be (or has been) selected to construct another centrifugal device of different fundamental design.

The NBS has inspected the Convair centrifugal device from a cryogenic aspect. The foreseeable problem areas have been mentioned. These problems are primarily shaft seals and reliable bearings. Brief laboratory experiments (described elsewhere in this report) have been performed to study the feasibility of ball bearings in such an application. Although shaft seals by others have performed with a good degree of success, there is reason to doubt high reliability. The "conventional" shaft seal used for cryogenic applications (booster pumps, etc.) are usually composed of graphite riding on a chrome plated stainless steel disc. The wear and deterioration of graphite over relatively long periods of time, when not lubricated, has been observed. A more extensive investigation to substantiate reliability may be beneficial.

3.5 Safety

Because of the need to meet definite schedules on a program, proper attention is often not given to safety. The safety procedures at Convair Astronautics - Centaur Project, and LASL - Rover Project, have not been reviewed in detail by the CEL staff. In a cursory inspection of the Convair facilities, no unsafe practices were observed. It would seem advisable however, to review the test facilities and procedures in greater detail, observe a tanking operation at Point Loma and eventually review procedures and operations at other test facilities planned by Convair. LASL personnel have requested an independent inspection of their Rover facilities, to help guarantee that all conceivable safety precautions have been taken.

The NBS staff has been called upon by many agencies of Government and Industry to give advice on both new and existing hydrogen facilities. Our staff is well acquainted with safety studies made by others and safety procedures taken by many laboratories in addition to our own intensive program to assure safe operations at CEL facilities.

3.6 Charts of Thermodynamic Properties of Hydrogen

Edmund H. Brown

Although the number of charts available on the thermodynamic properties of hydrogen is not large, the design engineer can obtain several of them which are at least partially contradictory and for which he usually has neither the time nor additional information required for a critical comparison. The purpose of this section is to make some brief comments on both the published and unpublished charts presently being used or circulated in the cryogenic industry with a view to assisting the engineer who is faced with such a choice.

Published charts for normal hydrogen include the three temperature-entropy diagrams in:

1. Keesom and Houthoff, Leiden Comm. Suppl. 65d (1928)
2. Woolley, Scott, Brickwedde, NBS J. Research 41 (1948)
3. W. Koeppe, Kaltetechnik 9 (1956)

In addition, the following unpublished diagrams have had some circulation in industry:

4. Temperature-Entropy diagram entitled "Hydrogen-Normal" NACA File No. 4842 (1958)
5. Enthalpy-Pressure diagram "for parahydrogen", no further identification, prepared by Dr. H. L. Johnston (on 3 sheets covering the range 0 to 200 atm.)

A recent Russian temperature-entropy diagram has been reported, but whether it is a partial revision of earlier diagrams or represents new data is unknown since copies have been unobtainable.

Most of the following comments are restricted to several key points which, although they cannot be used to demonstrate the reliability or accuracy of a given chart, can be used for the converse -- that is, to conclude that a particular chart contains sufficient inaccuracies that its use for design should not be seriously considered. These points include the following:

a. no isochore can intersect the (Joule-Thomson) inversion curve more than once;
b. the pressure component of the curvature vector of the inversion curve in a ln p - ln T diagram must be everywhere negative;
c. the low-temperature terminal point of the inversion curve must lie in the saturated liquid between the triple point and the critical point;
d. the slope of the isenthalps in a T-s diagram must be everywhere negative in the two-phase (liquid-vapor or solid-vapor) region;
e. both the temperature and entropy components of the curvature vector of the isenthalps in a T-s diagram must be everywhere positive in the two-phase region;
f. the enthalpy of the saturated vapor must pass through a maximum at some pressure below the critical pressure.

Some of the above conditions are discussed in

6. E. H. Brown, On the thermodynamic properties of fluids, Proc. 1960 Session Comm. I of the Int. Inst. of Refr. (to appear);

the remainder will be discussed briefly here.

The early Leiden diagram (1) of Keesom and Houthoff appears to satisfy all the above conditions. Actually there are two low-temperature diagrams in this article; in the second (or "corrected" diagram) the isenthalps in the compressed-liquid region are slightly

flatter than the original. In both, the enthalpy of the saturated vapor passes through a maximum at about 3.5 atm. The temperature at which the inversion curve terminates in the saturated liquid is approximately 27°K in the original diagram, and slightly lower (perhaps as low as 26°K) in the "corrected" diagram.

The diagram (2) of Woolley, Scott, Brickwedde is generally similar to the Leiden diagram (1) and also appears to satisfy all the above conditions. Since this later diagram contains considerable newer data and is the result of a wider and more careful correlation of data, some preference should be given for its use rather than (1); also, it is more readily available.

The recent T-s chart due to Koeppe (3) has been discussed in some detail in (6). The inversion curve passes through the point 55°K, 95 atm. with nearly the same slope as the 500 Amagat isochore which lies about 2°K above this point; thus, only a slight extrapolation to higher density is needed to show that in this region conditions (a) will be violated. Condition (b) is violated by all the points representing Koeppe's own data; the only points not showing a positive curvature are those from the (also probably incorrect) correlation by Baehr of early J-T measurements of Johnston, Bezman, and Hood. The inversion curve appears to wander off in the general direction of the fluid-solid phase transformation curve; thus, condition (c) is probably violated. Although conditions (d) and (e) are satisfied, condition (f) is not -- there is no sign of a maximum in the enthalpy of the saturated vapor, at least to pressures below one atm. Because of these many inaccuracies and irregularities, use of Koeppe's diagram (3) cannot be recommended.

The ubiquitous NACA temperature-entropy chart appears to have been widely circulated in the missile industry despite the fact that it is clearly marked "data not checked" and contains many obvious inaccuracies. In addition to the 210 BTU/lb. isenthalp being carelessly drawn and inconsistent with neighboring isenthalps, the following features can be noted: the smallest isenthalp included shows a clear maximum at 42.2°R or 23.4°K and the extrapolated terminal point of the inversion curve is at about 35°R or 19.5°K, a temperature far below the approximate 27°K indicated by other reliable charts as well as all the recent data; both conditions (d) and (e) are violated in parts of the two-phase region. Because of the importance of these latter conditions to the analysis of this chart, we shall give a sketch of their proof here.

From the First Law of thermodynamics in the form

$$Tds = dh - vdp$$

we can immediately write

$$\left(\frac{\partial s}{\partial T}\right)_h = \left(\frac{\partial p}{\partial T}\right)_h \left(\frac{\partial s}{\partial p}\right)_h = -\frac{v}{T}\left(\frac{\partial p}{\partial T}\right)_h.$$

For isenthalps within the two-phase region, however, $\left(\frac{\partial p}{\partial T}\right)_h = \left(\frac{dp}{dT}\right)_\phi$, where $\phi(p, T) = 0$ is the equation of the vapor-pressure curve. Since $\left(\frac{dp}{dT}\right)_\phi$ is always positive, the slopes of the isenthalps $\left(\frac{\partial s}{\partial T}\right)_h$ or $\left(\frac{\partial T}{\partial s}\right)_h$ must always be negative. Again, from the First Law,

$$\left[\frac{\partial}{\partial T} T \left(\frac{\partial s}{\partial T}\right)_h\right]_h = -\left[\frac{\partial}{\partial T} v \left(\frac{\partial p}{\partial T}\right)_h\right]_h = -\left[\frac{\partial}{\partial T} z \left(\frac{\partial \ln p}{\partial \ln T}\right)_h\right]_h,$$

or

$$T\left(\frac{\partial^2 s}{\partial T^2}\right)_h = \frac{v}{T}\left(\frac{dp}{dT}\right)_\phi - \frac{z}{T}\left[\frac{d^2 \ln p}{d(\ln T)^2}\right]_\phi - \left(\frac{d \ln p}{d \ln T}\right)_\phi \left(\frac{\partial z}{\partial T}\right)_h.$$

The first term on the right-hand side of the above expression is again positive, as is the third term, since $\left(\frac{\partial z}{\partial T}\right)_h$ must be negative in the two-phase region. In the following article:

7. L. Riedel, Kaltetechnik 9 (1957)

it is shown that the "logarithmic curvature" of the vapor-pressure curve is always negative for almost all substances (particularly for hydrogen). The exceptions, such as for water, occur only in close neighborhoods of the critical point; even here, the validity of the exception is far from certain due to the uncertainty in the critical temperature (this temperature can be lowered approximately one-half degree by solution of quartz in water). Therefore, the curvature components $\left(\frac{\partial^2 s}{\partial T^2}\right)_h$ and $\left(\frac{\partial^2 T}{\partial s^2}\right)_h = -\left(\frac{\partial T}{\partial s}\right)_h^3 \left(\frac{\partial^2 s}{\partial T^2}\right)_h$ must both be positive.

Because of such gross irregularities, the NACA diagram (4) should not be used for design calculations.

The final diagram (5), an unpublished enthalpy-pressure chart due to H. L. Johnston, is believed by us to be the result of applying an approximate method of correction to Johnston's data for normal hydrogen to obtain thermal properties of parahydrogen. This approximate method will be discussed briefly below. The diagram, itself, appears to satisfy all the conditions given above. In particular, the terminal point of the inversion curve appears to be only slightly above 27°K. This inversion curve and some of the others referred to previously are shown in Figure 13.

It is sometimes claimed that, in the method of calculating thermodynamic functions from the radial distribution function, statistical mechanics obtains the result that the derivatives of the density with respect to pressure are independent of the internal molecular states. This "result" is false in that it is actually equivalent to an assumption introduced at the beginning of all statistical mechanical treatments: that the Hamiltonian is separable into an internal and an external part. Nevertheless, as an ad hoc assumption, relatively good approximations may be obtained by this method, as evidenced by the fact that at 20°K the densities of normal and parahydrogen differ by only 1/2 percent, according to data from

8. R. B. Scott, Cryogenic Engineering, D. van Nostrand (1959)

If h(p, T) is the enthalpy at given pressure and temperature and $h^\circ(T)$ is the enthalpy of the ideal gas, the assumption of separability of internal and external states implies that the quantity $h(p, T) - h^\circ(T)$ is independent of ortho-para composition. By using the perfect gas enthalpy differences tabulated in (2), approximate calculations for parahydrogen can be made from normal hydrogen data: explicitly, the enthalpy of parahydrogen will be given by the approximation

$$h_{(para)}(p, T) = h_{(normal)}(p, T) - H^\circ(T)$$

where $H^\circ(T)$ is the "heat of conversion" of the perfect gas from the normal mixture to parahydrogen. Other thermal properties, such as the specific heat cp of parahydrogen can also be obtained from this approximation by well-known relations.

In conclusion, use of either the diagram (2) together with the above correction, or the unpublished chart (5) (if available) should give the most accurate results in calculations with parahydrogen.

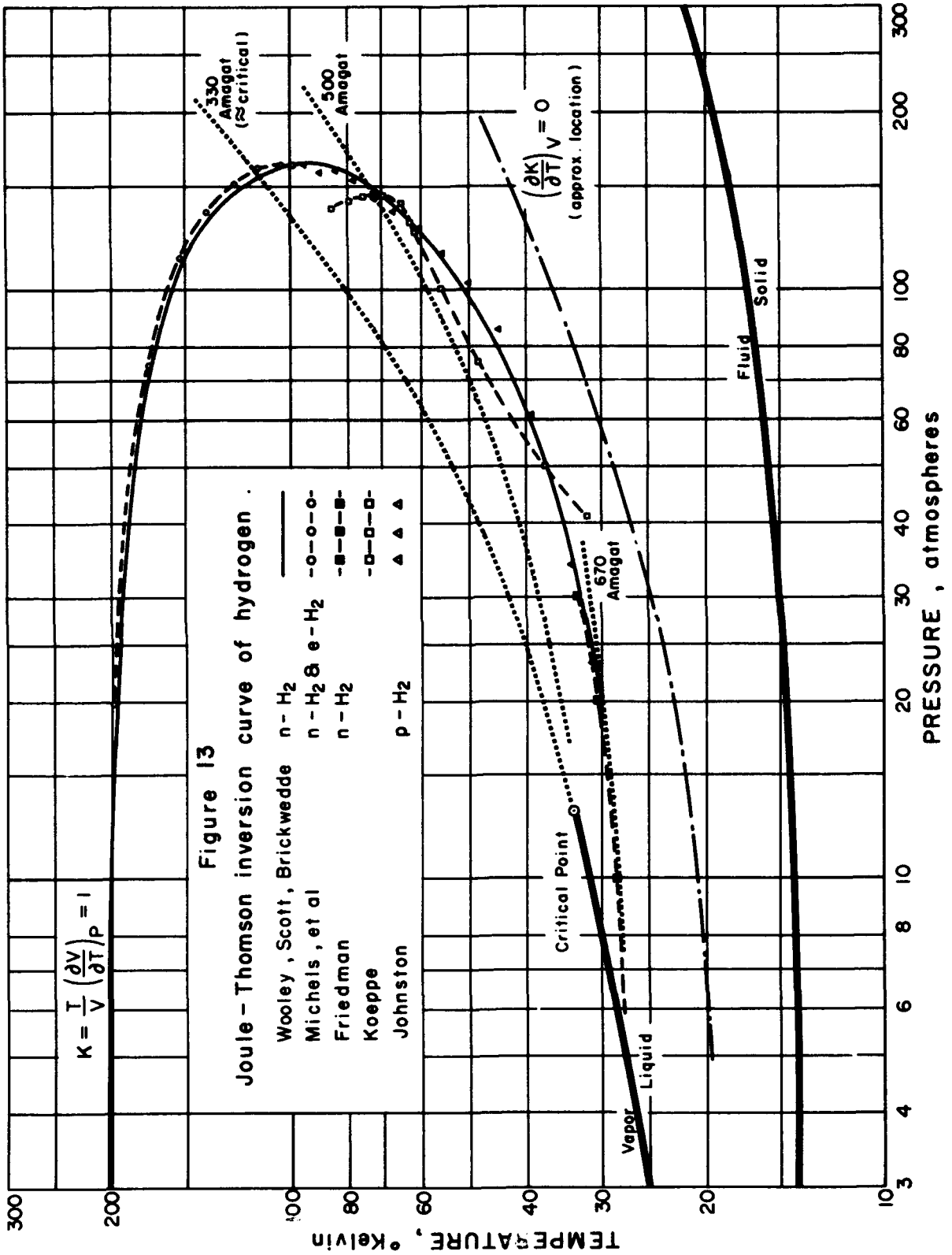

However, either course should be considered a stop-gap until the PVT data presently being obtained directly on parahydrogen at NBS-CEL can be used to prepare a new temperature-entropy diagram.

3.7 Conclusions

It is planned to make regular visits to Convair in the future to provide assistance on Project Centaur's cryogenic engineering problems in any way possible. In addition, visits are planned to other installations that might be concerned with cryogenic engineering problems relating to Projects Centaur, Rover and Saturn. It is not expected that the problems arising from these visits will be greatly different from those already encountered, however, such visits should serve to strengthen coordination of the cryogenic engineering effort on all of these projects.

Appendix I

The Thermal Properties of Gaseous and Liquid Hydrogen Below 60°K. A Preliminary Analysis of the Existent Data - W. T. Ziegler

Summary

A literature survey covering the period 1940-1956, prepared by Mr. R. H. Kropschot, has been used to determine whatis known about the thermal properties of liquid and gaseous hydrogen below 60°K. The excellent summary prepared by Woolley, Scott and Brickwedde [1] was assumed to represent the best available information prior to about 1944.

The literature search revealed that there was available extensive new data, most of it the work of H. L. Johnston and his co-workers at Ohio State University. These new data permit the construction of P-V-T and thermodynamic property charts for the liquid region from 20° to approximately the critical temperature, 33.2°K, for pressure up to 100 atm. The limited amount of earlier data by Bartholomé[10] permit the extension of these charts to 14°K.

Comparisons have been made of the compressibility factors, Z, observed by Johnston et al. with those obtained from RP1932 [1] for several isotherms. In general the compressibility factors observed by Johnston were lower than those calculated from RP1932 (Table 13). The maximum discrepancy noted was about 2 per cent, in the range 20 - 60° for an Amagat density up to 500. In the range below 20 - 35°K the P-V-T data of Johnston et al. is much more extensive than the Leiden data available at the time RP1932 was written.

The heat capacity, C_p, for liquid hydrogen has been shown to be in good agreement with the experimental data of Gutsche [24] near 20°K but the data of Gutsche appears to be approximately 10 - 15 per cent too large near 30°K, in agreement with the conclusions expressed in RP1932.

Values for C_p vs ρ at constant T and P have been calculated using RP1932 and the behavior of C_p and C_v in the critical region have been discussed.

The thermodynamic properties calculated by Johnston et al. from the P-V-T data have been compared with RP1932.

The present study is by no means a complete one. However, it is felt that certain ideas on which future study should concentrate have been determined.

Introduction

The present study is the result of a project to experimentally determine new data and to re-examine existing data available on the thermal and transport properties of gaseous, and liquid hydrogen over the range 14-60° and up to approximately 100 atm pressure. The excellent survey and compilation of the properties of hydrogen by Woolley, Scott, and Brickwedde [1] (hereafter referred to as RP1932) constituted the point of departure of the re-examination. Mr. R. H. Kropschot has made a literature survey for 1940-1955 in Chemical Abstracts and 1940-1956 in Physics Abstracts covering the areas of thermal properties, viscosity and thermal conductivity. For the years preceding 1940 the bibliography of RP1932 has been relied upon, although a number of other earlier papers have been examined for original data.

The present study is concerned only with the thermal properties of liquid and gaseous hydrogen. In all instances the word hydrogen implies "normal" hydrogen (75 per cent ortho, 25 per cent para) unless otherwise stipulated. In the earlier work on hydrogen the ortho-para composition is unknown; it is assumed to be for normal hydrogen.

The properties which are discussed have been grouped under the following broad headings:

P-V-T relations for gaseous and liquid hydrogen
Vapor pressure
Critical constants
Joule-Thomson effect
Heat capacity
Velocity of sound and relation to C_p/C_v
Thermodynamic properties

A more detailed listing is given in the Table of Contents.

Time available has not permitted a critical analysis of the data available in these areas. However, an attempt has been made to determine the probable effect of the newer data on the conclusions reached in RP1932, to indicate where new calculations are likely to be useful, and to determine where new experimental studies should be undertaken.

Much of the data on the thermal properties of hydrogen which has appeared since RP1932 was completed are the result of the extensive investigations of H. L. Johnston and his coworkers at Ohio State University. Much of this work has been reported in Technical Reports rather than in the open literature. In other reports little effort has been made by the authors to analyze the results critically with respect to existing data. The work of Johnston, et al. represents a considerable extension of the data available in '42-46 when RP1932 was being written, Thus, P-V-T data for the liquid in the range 20-33°K for pressures of 2-100 atmospheres, P-V-T data for gaseous hydrogen below 33°K, the heat capacity from the boiling to the critical point constitute information which for the most part was unknown in 1942-46.

One of the problems which arises in the combination of data from various sources is that of the absolute temperature scale used by the different investigators. The temperature scale used throughout the present paper has for its ice point T_o = 273.16° (the NBS scale of RP1932). Much of the Leiden data is given in the absolute centigrade scale with T = 273.09°K. Where necessary, the corresponding temperature on the scale with T_o = 273.16°K was obtained from the relation.

$$T_{NBS} = \frac{273.16}{273.09} \left(273.09 + t°C \right)$$

This method of conversion was used by Woolley et al [1] (conversation with R. B. Scott). All temperatures unless other specified refer to °K on this scale.

P-V-T Relations

a. Gas

The P-V-T relations for gaseous hydrogen prior to about 1946 have been summarized in Fig. 6 of Reference [1] and used to construct the Z vs ρ, T table of this work (RP1932). Examination of Fig. 6 shows that all these data were the result of measurements made at Leiden. The original Leiden data below 60.35°K has been reexamined [6] and a summary of it collected in Table I.

Since 1946 a large amount of additional data in the form of approximately 30 isotherms extending from 20 to 300°K and 1 to 200 atmospheres has appeared [7, 8, 10]. Fifteen of these isotherms are for temperatures in the range 20-60°K, seven of them being below the critical temperature (33.24°K). The data are summarized in Table II. This new work is the result of investigations of H. L. Johnston and coworkers at Ohio State University. It will be referred to hereafter as by Johnston. Johnston [8] has fitted virial equations of the form

$$\frac{PV}{RT} = Z = 1 + \frac{B}{V} + \frac{C}{V^2} + \frac{D}{V^3} + \frac{E}{V^4} + \frac{F}{V^5} \qquad (1)$$

to his isotherms for T ≥ 35.10°K and compared $Z_{obs} - Z_{calc}$ over the range of his data. He states [8, p 4] that "it is evident that the representation of these data by the virial equation yields results which, on the average, are in agreement with the experimental data to one part in 1000, or better, except at the lowest temperatures." At 33.96°K it was found impossible to fit the data to the six-term virial equation. For temperature T ≤ 33.00°K Johnston [7] uses fewer virial coefficients and does not explicitly give the comparison $Z_{obs} - Z_{calc}$. In none of these papers is a comparison made between the Leiden data, the Z vs ρ , T data in RP1932 and the Johnston results. However, it is clear that the Johnston data is much more extensive in the range T< ~35°K than is the Leiden data.

A few isotherms very near the critical point have also been measured by Hoge and Lassiter [8].

TABLE I

Isotherm t°C	T°K (RP1932)	Range of Amagat density,	Points in data	Leiden Comm. No.
-212.82	60.35	74-194	6	100a
		157-325	5	97a,99a
		70-90	3	165b
-217.41	55.77	78-195	6	100a
		285-359	3	97a,99a
		70-90	7	165b
		202-344	7	172a
-225.37	47.74	69-90	3	165b
		224-455	8	172a
		16-25	4	188e
-231.38	41.70	72-89	3	165b
		246-533	14	172a
		16-25	4	188e
-236.56		16-25	5	188e
-236.29	36.79	75-89	4	165b
		268-602	13	172a
-238.29	34.81	80-88	3	165b
		283-60	12	172a
-239.90	33.19	79-89	5	165b
		298-700	22	172a
-241.87	31.22	79-89	5	165b
		16-24	4	188e
-243.88	29.21	80-90	7	165b
-248.32	24.77	19-25	4	188e

TABLE II

Isotherm T °K	Pressure range atm	Amagat density, ρ, range	Reference
20.59	0.20 - 0.99	2.8 - 14.3	[7]
22.58	0.40 - 1.67	5.1 - 23.2	7
24.65	0.26 - 2.6	3.0 - 35.1	7
26.75	0.51 - 4.0	5.3 - 53.1	7
28.83	0.58 - 6.0	5.6 - 82.3	7
30.86	0.49 - 8.45	4.4 - 120.8	7
33.00	0.98 - 11.5	8.4 - 178.0	7
33.24(T_c)			
33.96	4.0 - 196.2	44.9 - 859	8
35.10	0.98 - 14.3	7.8 - 210	7
	16.2 - 190.7	367.2 - 843	8
37.61	5.4 - 199.5	6.6 - 190	8
40.09	0.95 - 17.9	6.6 - 190	7
	23.8 - 200.1	300.5 - 820	8
45.10	0.9 - 17.2	8.1 - 130.6	7
	22.8 - 202.8	190 - 783	8
50.09	2.06 - 16:2	11.4 - 102.3	7
	22.8 - 200	153 - 744	8
55.09	0.97 - 16.6	4.8 - 91.7	7
	23.6 - 198.6	136 - 704	8
60.03	0.93 - 30.5	4.2 - 158	7
	39.8 - 195.7	211 - 665	8
63.96	17.5 - 203	80.7 - 647	8

Intercomparison of Johnston data with RP1932 and Leiden data. This intercomparison was carried out at selected temperatures, and pressures in order to determine how closely the new Johnston data fitted the Z vs ρ, T table given in RP1932. Certain isotherms taken from the original Leiden data were also compared with the Table 13 in RP1932 to determine how well this Table reproduced the original Leiden data on which it was based. All comparisons have been made below ~60°K. In order to make this comparison the Amagat density corresponding to all points for T $\leq$ 63.96° of the Johnston data have been calculated using the relation

$$\rho = \frac{P V_o}{(PV)} \qquad (2)$$

$$Z = \frac{PV}{RT} \qquad (3)$$

where P and PV are given by HLJ in atm and cc. atm mole $^{-1}$, respectively. The value of R used by Johnston was R = 82.05667 cm^3 atm deg^{-1} [8, p. 3]. The value of V_o [the molal volume of 0°C and 1 atm pressure] used was 22428.5 cm^3 mole $^{-1}$, taken from RP1932, p. 396. Z has been calculated by Eq. (3) where this had not been done by Johnston.

The intercomparisons have been carried out in two ways. In the high density range, $\rho > 200$, T < 56°K, the comparison was made by four-point Lagrangian interpolation in the Table 13 of RP1932. In the low density region, $\rho < 200$, T < 56°K, the intercomparison has been carried out by means of the relation

$$\frac{T^{3/2}}{\rho}\left(1-\frac{PV}{RT}\right) = A + C\rho \qquad (4)$$

where A and C have been taken from Table 19 of RP1932. Eq. (4) provided a simple means of obtaining $\frac{PV}{RT}$ since the Table 13 is calculated from Eq. (4) together with Table 19 [see remarks in RP1932, p. 430].

High density range, $\rho > 200$. Z has been calculated from Table 13 for each point on the Johnston isotherms T = 45.10°, 37.61°K, as a function of ρ and the difference $Z_{NBS} - Z_{obs}$ plotted in Fig. 1. A similar comparison has been made for Leiden isotherms T = 47.74° and T = 36.79° in order to examine the agreement between Table 13 and the Leiden data used to construct the Table 13 in this range. [Data for the 45.10°K isotherm of Johnston in the range $\rho < 200$ is included. It was calculated using equation (4) as described below].

Examination of Fig. 1 shows that $Z_{NBS} - Z_{obs}$ is less than 2×10^{-3} for all points except one of the Leiden data whereas the Johnston data gives $Z_{NBS} - Z_{obs}$ as large as 6×10^{-3}. There seems to be more scatter in the Johnston data, but also some indication of a trend for Z_{obs} (HLJ) to be systematically smaller at high ρ than the Leiden data. For instance at T = 37.61°K ρ = 474.16 Z_{NBS} = 0.4152 Z_{obs} (HLJ) = 0.40920, the Z observed by HLJ being 1.45 per cent low.

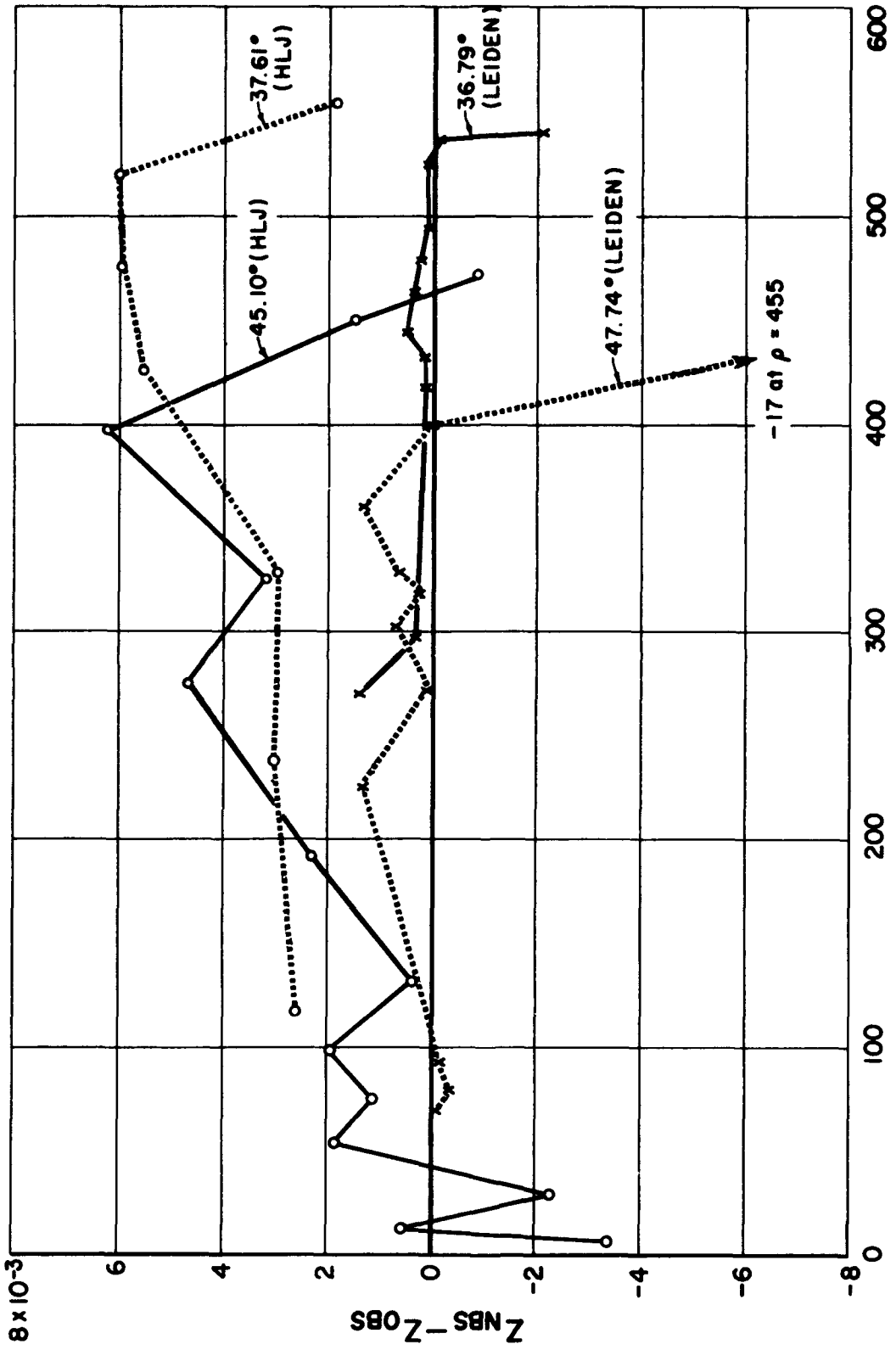

Figure 1
Comparison of Z_{NBS}-Z_{Leiden} and Z_{NBS}-Z_{HLJ} For approx. the same isotherms

Low density range, $\rho < 200$, $T < 56°K$. Z_{NBS} has been calculated as a function of ρ for all points given on the Johnston isotherms at $T = 20.59°$, $24.65°$, $26.75°$, $28.85°$, $30.86°$, $33.00°$ (all below $T_c = 33.24°$) and $35.10°$ and $45.10°$ using equation (4). Appropriate values of A and C for these temperatures were obtained by plotting the values of A and C given in Table 19 (RP1932). The difference $Z_{NBS} - Z_{obs}$ has been plotted vs ρ in Figure 2 for all isotherms. A similar comparison is shown for the Leiden isotherms at $T = 29.21°$, $31.22°$, $33.19°$, and $34.81°K$ in Figure 3.

It will be noted from Figure 3 that $Z_{NBS} - Z_{obs}$ is quite small for $T = 34.81°$ and $33.19°$. The agreement is less satisfactory for $T = 31.22°$ and $29.21°K$. This behavior is in agreement with conclusions to be drawn from Figure 9 (RP1932) p. 429, where the values of A and C′ for the first two isotherms fall on the curve used to obtain Table 19, while the experimental values of A for $T = 31.22$ and $29.21°$ fall off the smooth curve drawn, hence one would expect some disagreement between Table 13 and the Leiden data in this temperature range. It should be noted that these four isotherms represent a very limited range of ρ, whereas the Johnston data cover a much wider range of ρ. Examination of Figures 6 and 8 of RP1932 reveals how sparse the Leiden data really are in the temperature range 20-56° for $\rho < 200$.

Comparison of the Johnston data for Z with that calculated from RP1932, as shown in Figure 2, shows that as one goes from $20.59°$ to $45.10°$ the agreement between the two is good at $T = 20.59°$ where ρ is small (and limited by the saturation pressure), gets progressively poorer as T increases to about $33°K$ and then improves again. We may note that Z (for a given condition) of Johnston is almost invariably smaller than the corresponding Leiden value.

The percentage discrepancy between the Johnston data and the NBS Table 13 of RP1932 varies with the value of Z. At $T = 33.00°K$ where $Z \simeq 0.5$ Z_{HLJ} is 1.85 per cent smaller than Z_{NBS} for $\rho = 178$. This is the maximum discrepancy noted except for isolated points.

The possible effect of an error in the temperature measurement of the isotherm was examined at $33.00°K$. Decreasing the temperature to $32.90°$ improved the fit somewhat. It appears that the temperature would have to be decreased to about $32.6°$ to give the values of Zcalc from the NBS Table. Such an error in the temperature measurement seems highly unlikely in this temperature range.

One comparison of Johnston s data with his virial equation for $T = 30.86°$ and $P < P_{saturation}$ was made. The equation used as [7] .

$$\frac{PV}{RT} = 1 + \frac{B}{V} + \frac{C}{V^2} + \frac{D}{V^3}$$

where

$$B = -80.73 \text{ cc/mole}$$

$$C = 2078 \text{ (cc/mole)}^2$$

$$D = 30{,}000 \text{ (cc/mole)}^3$$

This equation was found to fit the experimental data to better than 2 parts per 1000 except at one point in the range $\rho \leq 120.8$. This fit is as good as can be obtained with equation (4).

It seems likely that the fit for other temperatures below $33°K$ will be equally good.

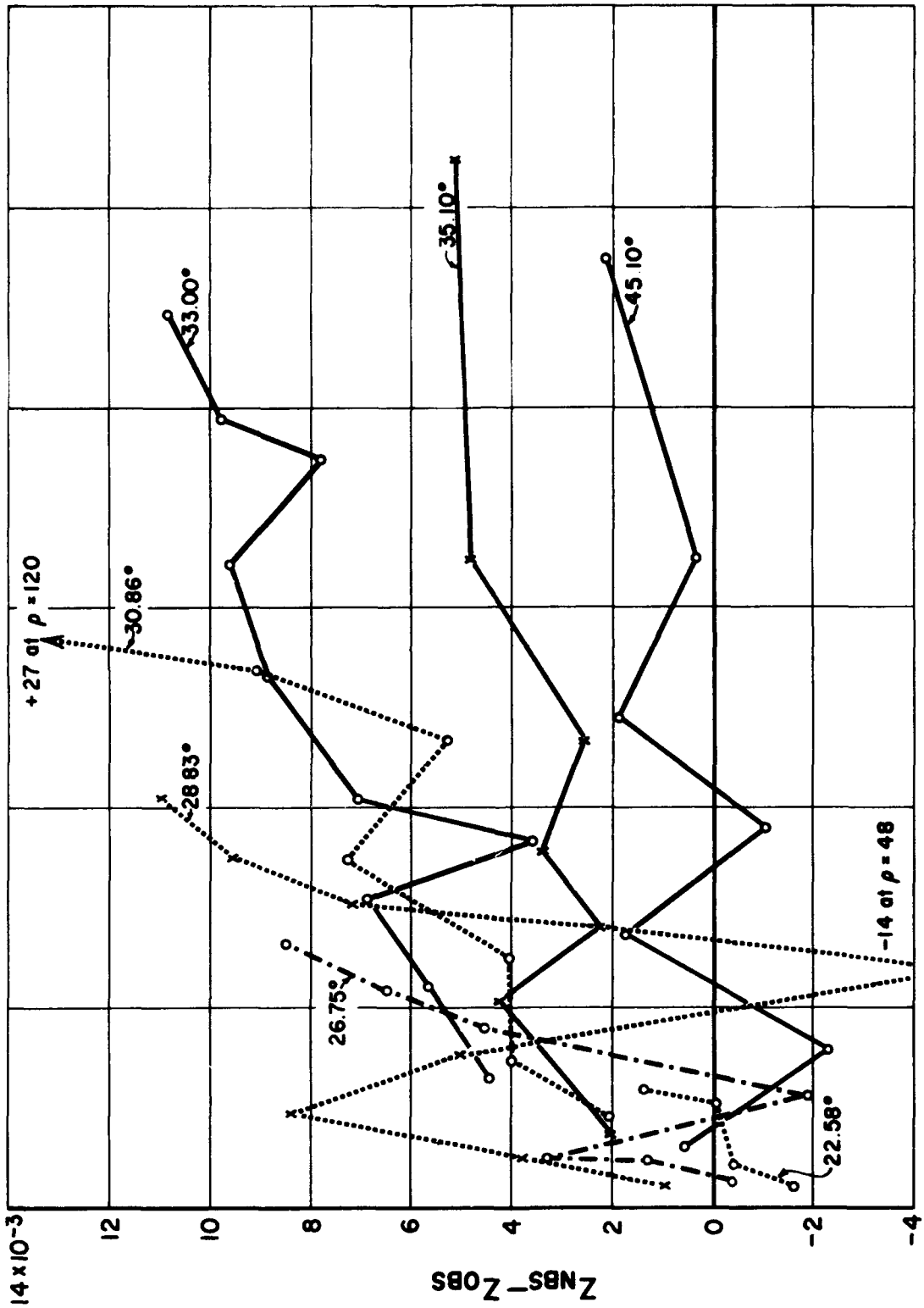

Figure 2
Comparison of Z_{NBS}-Z_{obs} (HLJ)

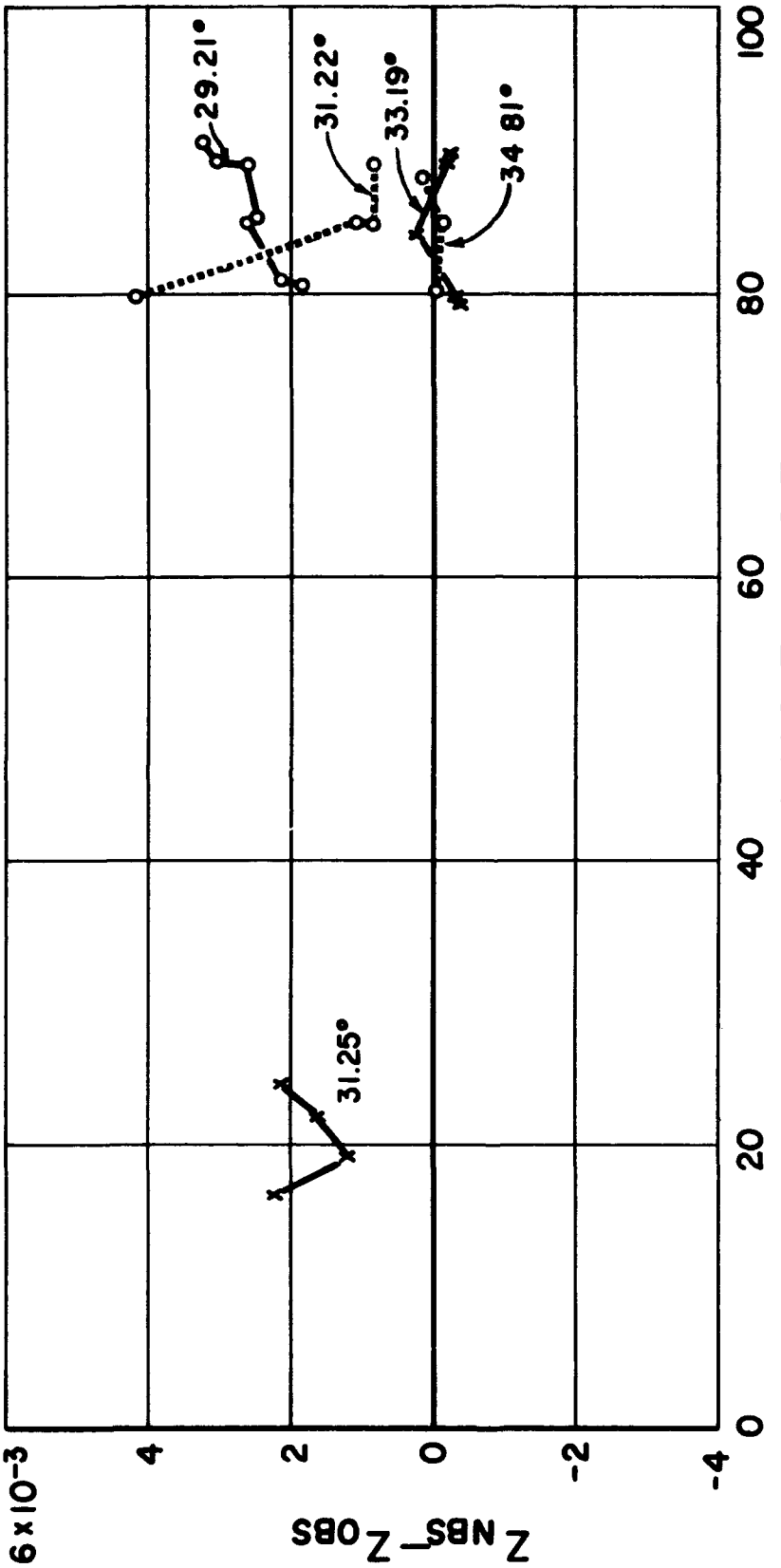

Figure 3
Comparison of Z_{NBS}-Z_{obs} (Leiden)

b. Liquid

The P-V-T relations for liquid hydrogen (n - H_2) in Reference 1 (RP1932) are based on the experimental measurements of Mathias, Crommelin, and Kamerlingh Onnes Leiden Comm. No. 1546b [12] for the saturated liquid over the range 20 - 33°K and upon the measurements of Bartholomé [10] for three isotherms having the following range of data:

$T_{°K}$	Pressure range range	Freezing pressure* atm
16.43	8 - 82	81.7
18.24	5 - 137.5	148.5
20.33	1 - 236.5	232.9

*Calc. from Equation 7.18, RP1932.

Since the appearance of RP1932, Johnston and his coworkers [9, 35] have measured the P-V-T relations for 9 isotherms covering the range 20.34° to 32.58°K from approximately 10 to 100 atmospheres. These results have been presented in the form of P vs T plots at constant V, and P vs V plots at constant T [9]. No new data were obtained for the volume of the saturated liquid; Johnston et al extrapolated their data to the saturation volumes given by Mathias et al cited above. Comparisons of Johnston's data for T = 20.38° with that of Bartholomé at T = 20.39° shows that the agreement is 1 per cent or better over the range 9 - 106 atm (where comparison is possible). Johnston et al [35] have extrapolated their volume data to 150 atm and have used their smoothed P-V-T data to calculate the thermodynamic properties of the liquid relative to the properties of the saturated liquid.

Friedman and Hilsenrath [3] have used Johnston's data [9] to prepare a table of T vs P values at constant V and compressibility factor Z vs P at constant V over the range 15 - 33°K. In a subsequent publication Friedman [4] has prepared a table of Z vs T at constant P over the range 16 - 33°K. In both instances the pressure goes to 120 atm.

c. Saturated vapor and liquid

No new data for the saturated vapor or liquid has appeared since the summary presented in RP 1932. It appears that the data given for n - H_2 (as liquid) in Table 31 p460 of RP1932 should be adequate. It should be noted that the data given for p - H_2 in Table 31 differ slightly from those for n - H_2.

Vapor Pressure Relations

n - H_2

White, Friedman, and Johnston [13] have recently measured the vapor pressure of n - H_2 from the boiling point to the critical point. In another paper they have measured T_c and P_c by the visual observation of the disappearance of the meniscus and found $T_c = 33.24_4$ °K and

P_c = 12.797 atm [19] .

They have expressed their measurements in the form of an equation

$$\log_{10} P_{atm} = a + \frac{b}{T} + cT + dT^2 \qquad (5)$$

which gives 20.40°K for the normal b.p. and P = 12.77$_3$ atm for T_c = 33.24$_4$°K. Comparison of this equation was made with one given in RP1932. At identical pressures the temperature calculated from each equation was compared. The difference in temperature $T_{HLJ} - T_{NBS}$ varied approximately linearly with T reaching +0.18° at the critical temperature. It should be pointed out that the equation from RP1932 is actually based on the range 14 - 20°K, but was stated (RP1932 p 454) to represent the Leiden data to the critical temperature (33.19°K) within the limits of experimental accuracy.

A detailed comparison of the Johnston and Leiden data should be made to determine the nature of the agreement directly. Grilly [16] has also reported the vapor pressure of n - H_2 to 3 atm pressure.

p - H_2

Hoge and Arnold [14] have recently measured the vapor pressures of p - H_2 (99.71 per cent p,0.21 per cent ortho), D_2 and HD from the normal b.p. to the critical point. Their experimental results have been expressed for p - H_2 in the form of a table permitting linear interpolation except above 30°K. It is interesting to note that Hoge and Lassiter [18] found the critical constants of p - H_2 to be T_c = 32.994°K, P_c = 12.770 atm, V_c = 65.5 cc/mole.

It should be noted that the vapor pressure of n - H_2 is slightly less at the same temperature than that of p - H_2 (see RP1932) for the range 14 - 20°K. Johnston's equation for n - H_2 [Equation 5 above] has this property at 20.4° and 32.994°K. It should be noted that o-p H_2 solutions do not follow the ideal solution laws [RP1932, Reference 14, 15, 17] .

Critical Constants

n - H_2

Woolley et al (RP1932) have summarized the critical constant data for n-H_2. The latest Leiden values as reported by Woolley et al are T_c = 33.19° (on the basis T_o = 273.16°) P_c = 12.751 atm and ρ_c = 344. (Amagat density). However, on the basis of the P-V-T data Woolley et al finally arrive at a compromise choice as follows:

T_c = 33.19° P_c = 12.98 atm ρ_c = 335 V_c = 66.95 cc/mole Z_c = 0.3191

More recently Johnston et al [19] have made a direct determination of the critical point by observing the disappearance of the meniscus. They report T_c = 33.24$_4$°K P_c = 12.797 atm.

p - H_2

Recently Hoge and Lassiter [18] have measured the critical constants of p - H_2 (99.71 per cent p, 0.21 per cent o), HD and e-D_2 using the isotherm method. Their results for p - H_2 are

$$T_c = 32.994°K \quad P_c = 12.770 \text{ atm} \quad V_c = 65.5 \text{ cc/mole} \quad Z_c = 0.309$$
$$\rho_c = 342.4$$

Joule-Thomson Effect

Johnston et al [20] have measured the Joule-Thomson effect in normal H_2 directly from 64°K and at room temperature. Most of the measurements were made in the range 64° - 80°K. The results of these measurements have been used by them [21] to calculate the thermodynamic quantities H-H°, $C_p - C_p°$ and S-S° over the range 65° - 300° and at even pressures from 5 to 200 atm.

Baehr has used the same data to calculate the quantities

$$\mu = \left(\frac{\partial T}{\partial P}\right)_H, \quad -\epsilon = \left(\frac{\partial H}{\partial P}\right)_T$$

and C_p over the range 60° to 85° from P = 0 to P = 180.

Both of these latter papers will be discussed in connection with the heat capacity and thermodynamic property section of this report.

Heat Capacity

The heat capacity of a substance may be expressed in a number of ways depending upon the particular process involved or the method of calculation used to obtain it. In this section we will discuss the following both for gaseous and liquid hydrogen:

$$C_p,\ C_v,\ C_p - C_p°,\ C_{p(satd.)},\ C_{satd.},\ C_p/C_v,\ C_v - C_v°.$$

Woolley et al (RP1932) have summarized the experimental data which consists of C_p measurements over the range 16.5 - 37°K and at seven pressures (11 - 99 kg/cm^2) by Gutsche [24] and C_v measurements by Eucken [26] and Bartholomé and Eucken [25] in the solid and liquid states. No new measurements have appeared for normal hydrogen. Johnston et al [23] have measured C_{satd} for liquid parahydrogen from 12.7° - 20.3°K and in a later paper have reported C_{satd} for liquid p-H_2 from the boiling point to the critical point [22].

Woolley et al (RP1932) have used their equation of state table, together with the experimental C_p data of Gutsche, to construct a plot of C_p vs T for several constant pressures for compressed gaseous and liquid hydrogen [their Fig. 27]. This Figure covers the range 15 - 42°K. Chelton et al[5]have used the equation of state data of RP1932 to calculate C_p for gaseous hydrogen over the range 20 - 300°K at constant pressures of 12.98 (P_c) 15, 20, 30, 40, 60, 100 atms. (Also, 1, 4.84 and 10 atm.) The data of Gutsche have been used to complete the Chart in the highly compressed fluid (liquid) region.

The extensive P-V-T measurements of Johnston and coworkers, together with the Joule-Thomson measurements of this group, and their recent heat capacity measurements on parahydrogen (liquid) permit one to obtain C_p by making use of appropriate thermo-dynamic relations. On the one hand, these calculations permit an independent check on the experimental measurements of Gutsche and, on the other, an independent check or comparison with the C_p results of Chelton, et al. [5] for the gas. An analysis of the curves of Chelton, et al. will be made from this point of view and the data of Gutsche compared with the calculations.

Some comments will also be made on the direct measurement of C_p and C_v, the behavior of C_p and C_v near the critical region, the measurement of C_p and C_v from velocity of sound measurements and the direct measurement of the C_p/C_v ratio.

a. C_p of gaseous n-H_2

1. Calculation from Joule-Thomson measurements

White and Johnston [36] have used the earlier Joule-Thomson measurements of White, Friedman and Johnston [20] from 65° - 300°K and 1 - 200 atm to calculate $H_p - H°$ at 5° intervals from 65° to 300°K and for 17 constant pressures from 2.5 to 200 atm. This Table was used to obtain $C_p - C_p°$ by linear interpolation. Combining these values of $C_p - C_p°$ with the values for $C_p°$ given by Hilsenrath et al [2] one can obtain C_p and compare the results with the calculation of C_p made by Chelton et al.

Baehr [21] has also used the Johnston J. T. data [20] to compute C_p over the range 60 - 85°K and o to 180 atm.

Comparison of the results of Johnston for C_p in the range 65° - 100°K was made at 40, 60, and 100 atm with the corresponding C_p results taken from the Chart of Chelton et al [5]. Down to 75°K the results agree to within about 3 per cent (0.2 cal/mole deg). At 70° the difference is 7.3 per cent for 100 atm, 3.8 per cent at 60 atm and 2 per cent at 40 atm, all lower than the Chelton values. The C_p values obtained by Baehr agree less well with the Chelton results than do those of Johnston.

It appears, therefore, that these J-T results of Johnston et al agree with the Chelton results reasonably well to about 70°K.

2. Calculations from Equation of State Data

Johnston and coworkers [34] have used their extensive P-V-T measurements for gaseous normal hydrogen to obtain $C_p - C_p°$ over the range 20 - 300°K for pressures from o to 200 atm. The results are presented in the form of a graph of $C_p - C_p°$ vs P for a series of isotherms. In the region of interest of this report the isotherms are 26, 28, 30, 32, 36, 38, 40, 45, 50, 55, 60, 65 and at 5° intervals to 100°K (thereafter at 10° intervals to 300°). Unfortunately no tabular data is presented so that $C_p - C_p°$ must be read from a graph.

These calculations were made by machine computation using the virial equation data to represent the P-V-T relations.

In the range 70 - 100°K and for pressures of 40, 60, and 100 atm the values of C_p calculated from the $C_p - C_p°$ graph of Johnston agree within about 3 per cent or better with the value derived by Chelton et al from the NBS P-V-T relations in RP1932. In the range 50 - 70° the agreement is within 6 per cent. However, the error in reading the Johnston plot [Fig. 2 of Reference 34] may be as much as 3 per cent.

For temperatures less than 50°K the agreement becomes progressively poorer. In fact, for $T < \sim 42°$, $C_p - C_p°$ becomes negative for pressures greater than 40-60 atmospheres. This is a clear indication of error in $C_p - C_p°$. In view of the general agreement observed between the Johnston and Leiden P-V-T data and the NBS P-V-T table in this region it seems probable that the reason for the discrepancy lies not in the P-V-T data itself, but in the failure of the virial equations to properly fit the P-V-T isotherm data. White and Johnston make no specific comments about this pecularity in $C_p - C_p°$ but do remark that "the calculated thermodynamic properties exhibited peculiarities arising from uncertainties in the derivatives of the virial coefficients [34]." In another place it is remarked by Johnston [8] that the representation of the compressibility factor data by the virial equations yields results which, on the average, are in agreement with the experimental data to one part in 1000 or better, except at the lowest temperatures. "At 33.96°K it was impossible to fit the data with a six-term virial equation. [8]"

For temperatures and pressures below $T_c \simeq 33.24°K$ and $P \leq P_c = 12.8$ atm we have earlier pointed out [see Section on P-V-T relations] that the Johnston P-V-T data is much more extensive than the Leiden data on which the Z vs ρ, T chart of RP1932 is based. Furthermore, there is a small but clear difference between the values of Z found by Johnston and those read from Table 13 of NBS RP1932 for the same p and T. This difference in P-V-T data may be expected to give $C_p - C_p°$ values which differ among themselves depending on the data used. The C_p vs T charts given by RP1932 [page 404] and by Chelton et al [5] show lines only for C_{psatd} vapor and C_p for p = 5 kg/cm² (4.84 atm), both calculated from the P-V-T data in RP1932.

b. C_p for liquid n-H_2

Heat capacity data for n-H_2 in the liquid state are rather sparse. The heat capacity of the saturated liquid, C_s, has been summarized for the range 14 - 20°K by Woolley et al [1] in their Table 37. No measurements of C_s for $T > \sim 22°K$ appear to have been made. Johnston and his coworkers have measured C_s for liquid p-H_2 over the range 14 - 20.3°K [23] and from 18.28° to 31.49°K [22] . The agreement between the values of C_s found by Johnston for p-H_2 and those given in RP1932 for n-H_2 is very good over the range 14 - 20°K. In the absence of data for n-H_2 above 20°K and because of the great similarity to be expected between n-H_2 and p-H_2 [the critical constants and vapor pressure curves are very nearly the same] it will be assumed that C_s for n-H_2 is the same at each temperature as that found by Johnston et al for p-H_2 over the

range 20 - 32°K.

Johnston et al [35] have used their earlier equation of state data for liquid n-H_2 [9] to calculate a table of values of $C_p - C_{p_{satd}}$ for P = 2 atm, to P = 150 atm at one degree intervals from T = 20°K to T = 33°K. In order to use this table to compute C_p it is necessary to have both $C_{p_{satd}}$ and C_s. Now the relation between these quantities is given by the relation [see for example Dodge, Chem. Eng. Thermodynamics, p. 252 ff]

$$C_s - C_{p_{satd}} = - T \left(\frac{\partial V}{\partial T}\right)_P \frac{dP}{dT} \qquad (6)$$

where $\left(\frac{\partial V}{\partial T}\right)_P$ is evaluated for the liquid at $T = T_s$, $P = P_s$ and $\frac{dP}{dT}$ = slope of the vapor pressure equation at T_s, P_s. Johnston, et al., [35] also give a table of the quantity

$$\frac{1}{V}\left(\frac{\partial V}{\partial T}\right)_P .$$

Thus, by combining the tabulated values given by Johnston, et al [35] for V, $\frac{1}{V}\left(\frac{\partial V}{\partial T}\right)_P$, and $C_p - C_{p_{satd}}$ with $\frac{dP}{dT}$ calculated from their vapor pressure equation for n-H_2 [13] one can calculate C_p for liquid hydrogen as a function of P and T. The calculation is summarized in the following Table III.

TABLE III

$T_{°K}$	P(satd) atm	$\frac{dP}{dT}$ $\frac{atm}{deg}$	V(satd) cc/mole	$\frac{1}{V}\left(\frac{\partial V}{\partial T}\right)_P$ deg-1	C_s	$C_s - C_{p_{satd}}$ Cal/mole °K	$C_{p_{satd}}$
20	0.90908	0.2798	28.27	0.0159	4.50	-0.218	4.72
22	1.5583	0.4033	29.24	0.0186	5.11	-0.290	5.40
24	2.5178	0.5613	30.39	0.0233	5.68	-0.412	6.09
26	3.8243	0.7512	31.94	0.0311	6.45	-0.625	7.08
28	5.5480	0.9801	33.91	0.0430	7.70	-0.989	8.69
30	7.7775	1.2593	37.03	0.0720	9.80	-1.957	11.74
32	10.628	1.6044			18		
33							
33.24							

One may compare the experimental results of Gutsche [24] with those obtained from the $C_p - C_{p_{satd}}$ tables of Johnston, et al. At 20°K the results are compared in the following Table IV.

TABLE IV

T = 20°K

P kg/cm^2	P atm	$C_p - C_{p_{satd}}$	C_p cal/mole °K Calc. from HLJ [35]	C_p cal/mole °K Gutsche (smooth curve)
	0.909 (V,P)	0	4.72	
11	10.65	-0.17	4.55	4.60
24	23.23	-0.36	4.36	4.46
40	38.72	-0.54	4.18	4.15
59	57.1	-0.72	4.00	3.96
79	76.46	-0.87	3.85	3.84
99	95.8	-1.00	3.72	3.68

These results are in remarkably good agreement, considering the fact that Gutsche estimates his results as accurate to ± 3 per cent. Similar comparisons have been made by me at 24°, 26°, 28° and 30°K. The agreement is poorer at the higher temperatures, the C_p values calculated from the Johnston Table being lower than measured by Gutsche by as much as 15 per cent. The results at T = 30°K are given in the following Table V.

TABLE V

P kg/cm^2	P atm	$C_p - C_{p_{satd}}$	C_p cal/mole °K Calc. from HLJ [35]	C_p cal/mole °K Gutsche (smooth curve)
	7.7775 (V,P)	0	11.74	
40	38.72	-5.63	6.11	7.05
59	57.1	-6.20	5.54	6.35
79	76.46	-6.51	5.23	5.70
99	95.8	-6.80	4.94	5.35

It is interesting to note that Woolley, et al., (RP1932, p. 465) concluded that Gutsche's values of C_p for liquid hydrogen were too high to be consistent with the best thermal and P-V-T data. They estimated that Gutsche's C_p values for liquid hydrogen were of the order of 15 per cent too high. The present analysis using Johnston, et al., [35] data and calculations suggest that near 20°K the Gutsche data are very nearly correct but do indeed become too high at higher temperatures.

It appears that a plot of C_p vs T over the range 20-30°K and P = saturation pressure to 150 atmospheres can be constructed quite readily. For T > 30°K the calculation will be more uncertain largely because C_s for the liquid varies rapidly with temperature. For T = 14° - 20° reliance must be placed on the limited P-V-T data of Bartholomé [10]. Since this agrees personably well with the data of Johnston, et al. [9] at 20.38°K, the C_p charts could probably be extended to ~100 atm in this region as well. Values of C_p could also be calculated from the NBS T-S diagram given in RP1932 by the relation

$$\left(\frac{\partial S}{\partial T}\right)_P = \frac{C_p}{T} = \text{slope of isobar} \qquad (7)$$

and the values of C_p so obtained compared with those calculated from the P-V-T data of Johnston, et al.

c. Calculation of $C_p - C_v$ and C_v

One may calculate these quantities from the relations given in RP1932 as follows:

$$\frac{C_p(\rho, T) - C_p^\circ(T)}{R} = -A - B + C - 1 \qquad \text{[Eq. 5.8 RP1932]}$$

$$\frac{C_v(\rho, T) - C_v^\circ(T)}{R} = -A - B \qquad \text{[Eq. 5.7 RP1932]}$$

where $A = 2\int_o^\rho \left[T\left(\frac{\partial Z}{\partial T}\right)_\rho / \rho\right] d\rho$

$$B = \int_o^\rho \left[T^2\left(\frac{\partial^2 Z}{\partial T^2}\right)_\rho / \rho\right] dp$$

$$C = \left\{\left[Z + T\left(\frac{\partial Z}{\partial T}\right)\right]_\rho^2 \Big/ \left[Z + \rho\left(\frac{\partial Z}{\partial \rho}\right)_T\right]\right\}$$

Thus,

$$\frac{C_p - C_v}{R} = C - 1 + \frac{C_p^\circ - C_v^\circ}{R} = C, \qquad (8)$$

and

$$C_v = C_p - RC \qquad (9)$$

Chelton, Macinko and Dean [5] have tabulated the quantities necessary to calculate C in the course of their calculating of C_p. Their values of

Z, $T\left(\frac{\partial Z}{\partial T}\right)_\rho$, $\rho\left(\frac{\partial Z}{\partial \rho}\right)_T$ and C_p have been used to obtain C_v by equation (9).

The final results are shown in the following Table VI.

TABLE VI

Comparison of C_p and C_v for n-H_2

T °K	ρ Amagat density	C_p Cal/mole°K	C_v
P = 40 atm			
70	168.271	6.545	3.177
60	211.98	7.426	3.140
50	301.09	9.751	3.239
46	368.81	11.494	3.223
44	415.21	12.106	3.198
42	467.53	11.754	3.111
P = 30 atm			
60	154.71	6.832	3.150
44	295.96	12.343	3.282
42	346.96	14.548	3.196
40	417.67	15.366	3.266
38	495.17	14.672	3.290
P = 20 atm			
44	167.23	8.935	3.198
40	219.29	13.156	3.322
38	278.49	20.547	3.475
36	418.30	34.575	3.58
P = 15 atm			
40	139.8	9.013	3.229
36	197.73	16.852	3.479
34	410.66	58.16	3.18

These calculations show that whereas C_p changes rapidly near the critical temperature for pressures less than 40 atm., C_v is almost constant at 3.2 cal/mole °K, very nearly the same value as $^vC_v°$.

Direct measurements of C_v for gaseous and liquid hydrogen have been reported by Eucken [26] over the range 18.6 - 47.5°K for a few constant values of the Amagat density (60 - 860). The following Table VII is a summary of his data given at even temperatures.

TABLE VII

C_v for gaseous H_2, cal/gm mole °K

T	C(moles/l.)	2.67[a]	4.89[a]	16.95	17.20	22.30	34.5	36.2
°K	ρ (Amagat density)	59.9	109.7	380.1	385.8	500.2	774	812
35		3.20	3.40 ca	4.5 ca	4.0	3.32	3.39	3.36
37.5		3.19	3.35	3.65	3.50	3.32	3.42	3.43
40		3.18	3.28	3.43	3.39	3.29		
45		3.14	3.30	3.30	3.30	3.68		

[a] Earlier work by Eucken, Berl. Sitzungsber. (1912) p. 144.

Eucken's results are for the most part in very good agreement with the results obtained from RP1932 and given in the preceding Table VI. Eucken states that the C_v appears to pass through a maximum in the neighborhood of the critical point ("in agreement with researches of Dieterici on other substances").

d. C_v for Liquid Hydrogen

C_v has been measured for liquid hydrogen by Eucken [26] and Bartholomé and Eucken [25] (according to RP1932) for a series of densities ranging from 380-860 Amagats. The relation between C_p and C_v is given by the expression

$$C_p - C_v = -T\left(\frac{\partial V}{\partial T}\right)_p \Big/ \left(\frac{\partial V}{\partial P}\right)_T \qquad (10)$$

Johnston, et al., [35] have tabulated V, $\frac{1}{V}\left(\frac{\partial V}{\partial T}\right)_p$, $-\frac{1}{V}\left(\frac{\partial V}{\partial P}\right)_T$

as a function of T at 1° intervals from 20-33°K and for pressures from 2-120 atm. These quantities, together with the C_p results obtained earlier for liquid H_2 could be used to calculate C_v. The computed values could

be compared with the results mentioned above [25, 26] .

e. Behavior of C_p and C_v Near the Critical Point

[Dodge, Chem. Engineering Thermodynamics p. 227ff gives many of the equations used in this section] .

The critical point is usually characterized by the two relations

$$\left(\frac{\partial V}{\partial P}\right)_{T_c} = \infty \quad , \left(\frac{\partial^2 V}{\partial P^2}\right)_{T_c} = \infty \tag{11}$$

or $$\left(\frac{\partial P}{\partial V}\right)_{T_c} = 0 \, , \left(\frac{\partial^2 P}{\partial V^2}\right)_{T_c} = 0$$

Now we may write

$$C_p - C_v = T\left(\frac{\partial V}{\partial T}\right)_P \left(\frac{\partial P}{\partial T}\right)_V \tag{12}$$

and since we can show (see below) that $\left(\frac{\partial P}{\partial T}\right)_V$ is finite and $\left(\frac{\partial V}{\partial T}\right)_P = \infty$ at $P = P_c$, $T = T_c$, $V = V_c$ it follows that (12) that

$$C_p - C_v = \infty \tag{13}$$

and either C_v is finite $C_p = \infty$ or C_p is an infinity of a higher order than C_v. Experimentally C_v is finite as we shall see.

f. The Nature of $\left(\frac{\partial P}{\partial T}\right)_V$

It is an experimental fact for gases that $\left(\frac{\partial P}{\partial T}\right)_V$ is very nearly a constant (i.e., the isometrics are linear) for all gases examined. The usual equations of state reflect this fact. For instance, for the van der Waal equation we find

$$\left(\frac{\partial P}{\partial T}\right)_V = \frac{R}{V - b} \tag{14}$$

whence $$\left(\frac{\partial^2 P}{\partial T^2}\right)_V = 0 \tag{15}$$

For the Beattie-Bridgeman Equation of state we find (Dodge, p. 220, eq. 5)

$$\left(\frac{\partial P}{\partial T}\right)_V = \frac{R}{V} + \frac{\alpha_o}{V^2} + \frac{\beta_o}{V^3} - \frac{\gamma_o}{V^4} \tag{16}$$

where α_o, β_o and γ_o are constants at fixed T.

We see that $\left(\frac{\partial P}{\partial T}\right)_{V = V_c}$ = finite at T_c.

We may also note that $\left(\frac{\partial^2 P}{\partial T^2}\right)_V \neq 0$ in general.

From the relation

$$\left(\frac{\partial V}{\partial T}\right)_P = - \frac{\left(\frac{\partial P}{\partial T}\right)_V}{\left(\frac{\partial P}{\partial V}\right)_T} \tag{17}$$

we conclude that $\left(\frac{\partial V}{\partial T}\right)_P = \infty$ at $T = T_c$, $P = P_c$, $V = V_c$.

The exact behavior of C_p for real gases as a function of T and P near the critical point has been studied experimentally for very few gases. The classic case is steam [See, for instance, Dodge, p. 226-7] . H_2 has been examined by Chelton, et al.[5] . The quantity $C_p - C_p^o$ has also been generalized by assuming the law of corresponding states [See, for instance, Hougen and Watson, Chem. Process Principles, Vol. 2, Dodge, p. 243, Lydersen Greenkorn and Hougen, Eng. Expt. Station Bull. No. 4, Univ. of Wisconsin (1955).]

g. Behavior of C_v in the Critical Region

We may write

$$\left(\frac{\partial C_v}{\partial V}\right)_T = T\left(\frac{\partial^2 P}{\partial T^2}\right)_V \tag{18}$$

$$\text{or } C_v (V, T) - C_v^o (V = \infty, T) = \int_{V=\infty}^{V} T\left(\frac{\partial^2 P}{\partial T^2}\right)_v dV \tag{19}$$

For a gas obeying van der Waal's equation of state we see that from Equation (15)

$$C_v (V, T) - C^o (V = \infty, T) = 0$$

$$\text{or} \qquad C_v (V, T) = C_v^o (V = \infty, T) \tag{20}$$

for all T and V including T_c, V_c.

Hence $C_v = f(T)$ only.

For the Beattie-Bridgeman equation of state (Dodge, p. 220) one can show that

$$\left(\frac{\partial^2 P}{\partial T^2}\right)_V = -\frac{6R_c}{T^4V^2}\left[1 + \frac{Bo}{V} - \frac{bBo}{V^2}\right] \qquad (21)$$

where C, B_o, b are empirical constants in the Beattie-Bridgeman equation of state. Consideration of the magnitude and sign of C, B_o and b for some of the common gases [see Table V-4, p. 185 Dodge] indicates that

$\left(\frac{\partial^2 P}{\partial T^2}\right)_V$ is small and negative

Hence $C_v - C_v^o > 0$.

In RP1932 one finds the exact expression, expressed in terms of the Amagat density

$$\frac{C_v\,(\rho, T)}{R}\,(\text{real gas}) - \frac{C_v^o\,(T)}{R}\,(\text{ideal gas}) = -2\int_0^\rho \left[T\left(\frac{\partial Z}{\partial T}\right)_\rho\right]\frac{d\rho}{\rho} - \int_0^\rho \left[T^2\left(\frac{\partial^2 Z}{\partial T^2}\right)_\rho\right]\frac{d\rho}{\rho} \qquad (22)$$

Woolley, et al. (RP1932) have tabulated $\left(\frac{\partial Z}{\partial T}\right)_\rho, \left(\frac{\partial^2 Z}{\partial T^2}\right)_\rho$ vs ρ and T.

We note that $\left(\frac{\partial Z}{\partial T}\right)_\rho > 0$ and $\left(\frac{\partial^2 Z}{\partial T^2}\right)_\rho < 0$ for all ρ (0-500).

Hence there are two opposing terms in Equation (22).

Writing Eq. (22) in the form

$$\frac{C_v - C_v^o}{RT} = \int_0^\rho \frac{1}{\rho}\left[-2\left(\frac{\partial Z}{\partial T}\right)_\rho - T\left(\frac{\partial^2 Z}{\partial T^2}\right)_\rho\right] d\rho = \int_0^\rho \frac{\Delta}{\rho}\, d\rho \qquad (23)$$

one finds that $\Delta > 0$ for $0 \leq \rho \leq \sim \rho_c \simeq 350$; $\Delta = 0$, $\rho \simeq 350$; $\Delta < 0$. for $350 \leq \rho \leq 500$ for T = 36°K. For T = 70°, 200°K, $\Delta > 0$ for $0 \leq \rho \leq 500$. [These are selected T's for calculation].

We note further that when $\Delta = 0$

$$\left(\frac{\partial C_v}{\partial \rho}\right)_T = 0, \text{ in this case a maximum.} \qquad (24)$$

The consequence of this is that $\left(\frac{\partial^2 p}{\partial T^2}\right)_V = 0$ also.

It is believed that a detailed analysis of C_v vs ρ at a series of isotherms near the critical (33.24°K) will show a series of maxima in the C_v vs ρ isotherms for H_2.

Michels, et al. [32, See also 31] have made a detailed analysis of C_v vs ρ for T = constant for C_v of CO_2 in the critical region. C_v was calculated by them from their equation of state data for CO_2. These curves show a maximum in C_v for CO_2 at the critical point ($C_v - C_v^o \simeq 11$ at T_c and ρ_c). The curious fact pointed out by Michels is that the maximum occurs at very nearly the critical density for all isotherms from t = 31.04° (= t_c) to temperatures as high as 150°C. Michels comments on the maxima observed in C_v and points out that this implies

$$\left(\frac{\partial C_v}{\partial \rho}\right)_T = 0 \text{ and } \left(\frac{\partial^2 p}{\partial T^2}\right)_V = 0 \quad \text{for } \rho = \rho \text{ crit.}$$

Michels further remarks that the maximum in C_v at the critical density was first observed by Keesom [32.1] (this article is not available to me) and remarks that Yound observed

$$\left(\frac{\partial^2 P}{\partial T^2}\right)_V = 0 \text{ for isopentane of the critical point. [32.2]}$$

[The variation of C_v with ρ at constant T for CO_2 is also discussed in earlier papers by Michels, et al] [32.3, 32.4]

It is interesting also to note that Eucken [26] has observed a maximum in C_v near the critical point which is (as he remarks without reference) "in agreement with the researches of Dieterici for other substances." (Eucken's results are given in Table VII of this paper.)

h. Generalization of $C_v - C_v^o$

We may write the following relations

$$H = E + PV = E + ZRT \tag{25}$$

or

$$\frac{E^o - E}{T_c} = \frac{H^o - H}{T_c} - (1 - Z)\, RT_R \tag{26}$$

Since the terms on the right are expressible in terms of T_R and P_R (See, for instance, engineering charts such as given by Dodge, p. 241), we may generalize

$$\frac{E^o - E}{T_c}.$$

Finally we may write

$$\left[\frac{\partial\left(\frac{E^\circ - E}{T_c}\right)}{\partial T}\right]_V = \frac{C_v^\circ - C_v}{T_c}$$

or

$$\left[\frac{\partial\left(\frac{E^\circ - E}{T_c}\right)}{\partial T_R}\right]_{V_R} = C_v^\circ - C_v \qquad (27)$$

Lydersen, Greenkorn and Hougen [37] give tables and one plot of $\frac{E^\circ - E}{T_c}$. However, they give no tables or plots for $C_v^\circ - C_v$.

1. Determination of C_p/C_v

Velocity of Sound Method. The velocity of sound can be related (for zero frequency) to the thermodynamic properties of a fluid by a number of relations, such as (Zemansky, p. 133)

$$a = \sqrt{\frac{\beta_s}{d}} \qquad \text{where } \beta_s = -\frac{1}{\frac{1}{v}\left(\frac{\partial V}{\partial P}\right)_s} = \frac{1}{K_s} \qquad (28)$$

$$d = \text{density} = \frac{M}{V}$$

We may also write for C_p/C_v the result

$$\frac{C_p}{C_v} = \frac{K_T}{K_s} = \frac{-\frac{1}{V}\left(\frac{\partial V}{\partial P}\right)_T}{-\frac{1}{V}\left(\frac{\partial V}{\partial P}\right)_s} \qquad (29)$$

These equations, together with other thermodynamic relations, yield the additional relations

$$\frac{C_p}{C_v} = \frac{-Ma^2}{V^2}\left(\frac{\partial V}{\partial P}\right)_T \qquad (30)$$

$$a^2 = -\frac{V^2}{M}\left(\frac{\partial P}{\partial V}\right)_T + \frac{V^2}{M}\,\frac{T}{C_v}\left(\frac{\partial P}{\partial T}\right)_v^2 \qquad (31)$$

The relation given in Equation (30) is interesting in that it relates the equation of state data for an isotherm to a^2, C_p and C_v in a very simple way.

Equation (31) is interesting since it gives a simple relation between a and other quantities at the critical point. Thus, when $T = T_c$, $V = V_c$

$\left(\frac{\partial P}{\partial V}\right)_T = 0$ and both C_v and $\left(\frac{\partial P}{\partial T}\right)_V$ are finite, therefore

$$a^2_{crit} = \frac{V_c^2}{C_{v(crit)} M}\left(\frac{\partial P}{\partial T}\right)^2_{V = V_c} \qquad (32)$$

Resonance Method of Measurement of C_p/C_v. The resonance method of measuring C_p/C_v is described briefly in Zemansky, Heat and Thermodynamics, 3rd Ed., p. 129ff. It apparently does not require any P-V-T data, but is a direct method. Such a method, if feasible for low temperature use, would be very useful as an independent check on C_p/C_v or as a means of obtaining C_p from measured C_v data. Several references to this method are given here [27, 28, 29, 30].

Thermodynamic Properties of Hydrogen

Johnston, et al. [36] have calculated the quantities $C_p - C_p^o$, $H^o - H$ and $S - S^o$ for gaseous hydrogen from their Joule-Thomson data for the range 65-300°K and for pressures from 2.5 to 200 atm. Baehr [21] has also used the Joule-Thomson data of Johnston, et al. [20] to calculate $C_p - C_p^o$ for the temperature range 60-85°K and for pressures from zero to 180 atm. Baehr has also calculated the adiabatic and isothermal J-T coefficients over the same ranges.

The heat capacity results of Johnston and Baehr have been discussed in the section of this paper which deals with heat capacity.

In a later paper Johnston, et al. [34] have computed $C_p - C_p^o$, $H^o - H$ and $S - S^o$ from their very extensive P-V-T which extends from 20-300°K and for pressures of one to 200 atm. The results are presented in a series of charts of Z vs P, T; $H^o - H$ vs P, T; and two H - S (Mollier) diagrams. Unfortunately the charts are difficult to read accurately because of the coarse grid. The $C_p - C_p^o$ results have been discussed in the section of this paper which deals with heat capacity. The values of $C_p - C_p^o$ given by Johnston, et al. are certainly incorrect in the range below about 42 K for pressures above 40-60 atmospheres, presumably because the virial equations used to represent the P-V-T data in this region do not accurately reproduce this data. This suggests that $H - H^o$ and $S - S^o$ may also be in error in this same region, though perhaps to a lesser extent

since only first derivatives are involved in the calculation of these quantities. Since the P-V-T data of Johnston, et al. deviate significantly from the corresponding values of $\underline{Z}$ obtained from RP1932, one will expect some disagreement between thethermodynamic quantity obtained by Woolley, et al. (RP1932) and Johnston, et al. [34] .

Johnston, et al. [35] have also used their P-V-T data for liquid n-H_2 [9] to compute V, $C_p - C_{p_{satd}}$, $H - H_{satd}$, $S - S_{satd}$, $-\frac{1}{V}\left(\frac{\partial V}{\partial P}\right)_T$, $\frac{1}{V}\left(\frac{\partial V}{\partial T}\right)_P$ over the range 20-33°K and 2-120 atm. The use of these quantities require that $C_{p_{satd}}$, H_{satd}, and S_{satd} be established. The calculation of $C_{p_{satd}}$ is discussed in the section on heat capacity. A detailed comparison of these quantities with RP1932 has not been made. However the values of C_p computed with the help of Johnston's $C_p - C_{p_{satd}}$ values agree with experimental error with the measurements of Gutsche [24] at 20°K for the range 9-96 atm. When RP1932 [1] was written no P-V-T data existed for the liquid range for T >21° except along the saturation line. It appears that the data and computed thermodynamic functions can be used to construct a much more adequate T-S diagram in this region.

Bibliography

General

1. Compilation of thermal properties of hydrogen in its various isotopic and ortho-para modifications, H. W. Woolley, R. B. Scott and F. G. Brickwedde, J. Research Nat. Bur. Standards, 41, 379 (1948)(RP1932)

2. Tables of Thermal Properties of Gases, J. Hilsenrath, et al., Nat. Bur. of Standards Circ. 564 (1955).

3. The thermodynamic and transport properties of liquid hydrogen and its isotopes, Part I, A. S. Friedman and J. Hilsenrath, NBS Report 3163, March 15, 1954.

4. Op. cit., Part II, A. S. Friedman, NBS Report 3282, May 1, 1954. Compressibility factors, viscosity, dielectric constant and surface tension.

5. Thermodynamic properties of hydrogen, D. B. Chelton, J. Macinko and J. Dean, NBS-CEL Laboratory Note, dated Nov. 14, 1956.

P-V-T Relations

6. Communications Univ. Leiden, No. 94a, 99a, 100a, 127c, 165b, 172a, 188e.

7. Low pressure P-V-T data of gaseous hydrogen from the boiling point to room temperature, D. White, A. S. Friedman, and H. L. Johnston, Contract W33-038-ac-14794 (16243), Techn. Rpt. TR-264-12 (no date given).

8. Gaseous data of state II, The pressure-volume-temperature relationships of gaseous normal hydrogen from the critical temperature to room temperature and up to 200 atmospheres pressure, H. L. Johnston, D. White, H. Wirth, C. Swanson, L. H. Jensen and A. S. Friedman, Contract W33-038-ac-14794 (16243) Tech. Rpt. No. TR-264-25, Nov. 25, 1953.

9. The compressibility of liquid normal hydrogen from the boiling point to the critical point at pressures up to 100 atmospheres, H. L. Johnston, W. E. Keller and A. S. Friedman, J. Am. Chem. Soc. 76, 1482 (1954).

10. Zur thermischen and Kalorischen Zustands Gleichung der Kondensierten Wasserstoffisotopen, E. Bartholomé, Z. Physik. Chem. [B] 33, 387 (1936).

11. Gaseous data of state for hydrogen between 1 and 200 atm. from 20 to 300°K, H. L. Johnston, I. I. Bezman, T. Rubin, L. Jensen, D. White and A. S. Friedman, Phys. Rev. 79, 235 (1950) (Abstract).

12. Communications Univ. Leiden No. 151c, 154b.

Vapor Pressure

13. Vapor pressure of normal hydrogen from the boiling point to the critical point, A. S. Friedman and H. L. Johnston, J. Am. Chem. Soc. 72, 3927 (1950).

14. Vapor pressures of hydrogen, deuterium and hydrogen deuteride and the dew-point pressures of their mixtures, H. J. Hoge and R. D. Arnold, J. Research, NBS 47, 63 (1951)(RP2228).

15. A test of the ideal solution laws for H_2, HD and D_2. Vapor pressures and critical constants of the individual components, R. D. Arnold and H. J. Hoge, J. Chem. Phys. 18, 1295 (1950).

16. The vapor pressures of hydrogen, deuterium and tritium up to three atmospheres, E. R. Grilly, J. Am. Chem. Soc. 73, 843 (1951).

17. Vapor pressure of parahydrogen and orthohydrogen mixtures, H. W. Woolley, NBS Report 3253, April 15, (1954).

Critical Constants

18. Critical temperatures, pressures and volumes of hydrogen, deuterium and hydrogen deuteride, H. J. Hoge and J. W. Lassiter, J. Research, NBS 47, 75 (1950)(RP2229).

19. Direct determination of the critical temperature and critical pressure of normal hydrogen, D. White, A. S. Friedman and H. L. Johnston, J. Am. Chem. Soc. 72, 3565 (1950).

Joule-Thomson Effect

20. Joule-Thomson effects in hydrogen at liquid air and at room temperatures, H. L. Johnston, I. I. Bezman and C. B. Hood, J. Am. Chem. Soc. 68, 2367(1946).

21. Zur Kenntnis des Joule-Thomson Effektes in Wasserstoff, H. D. Baehr, Z. Elektrochem. 59, 32 (1955).

Heat Capacity

22. Condensed gas calorimetry VI. The heat capacity of liquid para-hydrogen from the boiling point to the critical point. A. L. Smith, N. C. Hallett and H. L. Johnston, J. Am. Chem. Soc. 76, 1486 (1954).

23. Condensed gas calorimetry I. Heat capacity, latent heats and entropies of pure parahydrogen from 12.7-20.3°K, H. L. Johnston, J. T. Clarke, E. B. Rifkin and E. C. Kerr, J. Am. Chem. Soc. 72, 3933 (1950).

24. Thermische Messungen an flüssigem Wasserstoff, H. Gutsche, Z. physik. Chem. [A] 184, 45 (1939).

25. Die direkte calorimetrische Bestimmung von C_v der Wasserstoffisotopen im festem und flussigen Zustand, E. Bartholomé und A. Eucken, Z. Elektrochem. 42, 547 (1936).

26. Über das thermische Verhalten einiger Komprimierter und Kondensierter Gase bei tiefen Temperaturen, A. Eucken, Verh. deut. Phys. Gesells. 18, 4 (1916)

27. Resonance method of measuring the ratio of the specific heats C_p/C_v of a gas, A. L. Clark and L. Katz, Can. J. Research 21A, 1 (1943).

28. On the determination of the ratio of specific heats of gases by an electro-acoustic method, J. Bouchard, Compt. rend. 226, 1434 (1948).

29. The ratio of the specific heat of gases C_p/C_v by a method of self-sustained oscillations, W. F. Koehler, J. Chem. Phys. 18, 465 (1950).

30. Note on the resonance method of measuring the ratio of specific heats of a gas, C_p/C_v, H. W. Woolley, Can. J. Physics 31, 604 (1953).

31. Molecular Theory of Gases and Liquids, J. O. Hirschfelder, C. F. Curtiss and R. B. Bird. John Wiley and Sons, Inc., New York, N. Y. (1954), p. 367ff.

32. Thermodynamic Properties of CO_2 up to 3000 atmospheres between 25° and 150°C, A Michels, A. Bijl and C. Michels, Proc. Roy. Soc. (London) A160, 376 (1937).

32.1 W. H. Keesom, Leiden Comm. No. 88.
See also Dissertation, Leiden, p. 83 (1908)

32.2 S. Young, Proc. Phys. Soc. (London) 13, 602 (1895).

32.3 Isotherms of CO_2 between 0° and 150°C and pressures from 16 to 250 atmospheres (Amagat densities 18-206), A. Michels and Mrs. C. Michels, Proc. Roy. Soc. (London) 153A, 201 (1936).

32.4 Isotherms of CO_2 between 70 and 3000 atmospheres (Amagat densities between 200 and 600), A. Michels, Mrs. C. Michels and H. Wouters, ibid, 214 (1936).

Velocity of Sound

33. Velocity of sound in liquid hydrogen, A. Van Itterbeek and L. Verhagen, Nature, 163, 399 (1949). (See also Proc. Phys. Soc. (London), 62B, 62 (1949), Physica 20, 307 (1954).)

Thermodynamic Properties

34. The thermodynamic properties of gaseous hydrogen from experimental data of state, D. White and H. L. Johnston, Contract W33-038-ac-14794 (16243) Techn. Report TR- 54-26, Nov. 30, 1953.

35. The thermodynamic properties of liquid normal hydrogen between the boiling point and the critical temperature and up to 150 atmospheres pressure, D. White and H. L. Johnston, Contract W33-038-ac-14794 (16243). Techn. Report TR-264-23, February 1, 1953.

36. Computation of thermodynamic properties of compressed gaseous hydrogen based on Joule-Thomson effect measurements, D. White, H. L. Johnston and P. Camky, Contract W33-038-ac-14794(16243), Techn. Report TR 264-21, June 15, 1952.

37. Generalized Thermodynamic Properties of Fluids, A. L. Lydersen, R. A. Greenkorn, and O. A. Hougen, Engineering Expt. Station Report No. 4, University of Wisconsin (1955).

U.S. DEPARTMENT OF COMMERCE
Frederick H. Mueller, *Secretary*

NATIONAL BUREAU OF STANDARDS
A. V. Astin, *Director*

THE NATIONAL BUREAU OF STANDARDS

The scope of activities of the National Bureau of Standards at its major laboratories in Washington, D.C., and Boulder, Colo., is suggested in the following listing of the divisions and sections engaged in technical work. In general, each section carries out specialized research, development, and engineering in the field indicated by its title. A brief description of the activities, and of the resultant publications, appears on the inside of the front cover.

WASHINGTON, D.C.

ELECTRICITY. Resistance and Reactance. Electrochemistry. Electrical Instruments. Magnetic Measurements. Dielectrics.

METROLOGY. Photometry and Colorimetry. Refractometry. Photographic Research. Length. Engineering Metrology. Mass and Scale. Volumetry and Densimetry.

HEAT. Temperature Physics. Heat Measurements. Cryogenic Physics. Rheology. Molecular Kinetics. Free Radicals Research. Equation of State. Statistical Physics. Molecular Spectroscopy.

RADIATION PHYSICS. X-Ray. Radioactivity. Radiation Theory. High Energy Radiation. Radiological Equipment. Nucleonic Instrumentation. Neutron Physics.

CHEMISTRY. Surface Chemistry. Organic Chemistry. Analytical Chemistry. Inorganic Chemistry. Electrodeposition. Molecular Structure and Properties of Gases. Physical Chemistry. Thermochemistry. Spectrochemistry. Pure Substances.

MECHANICS. Sound. Pressure and Vacuum. Fluid Mechanics. Engineering Mechanics. Combustion Controls.

ORGANIC AND FIBROUS MATERIALS. Rubber. Textiles. Paper. Leather. Testing and Specifications. Polymer Structure. Plastics. Dental Research.

METALLURGY. Thermal Metallurgy. Chemical Metallurgy. Mechanical Metallurgy. Corrosion. Metal Physics.

MINERAL PRODUCTS. Engineering Ceramics. Glass. Refractories. Enameled Metals. Constitution and Microstructure.

BUILDING RESEARCH. Structural Engineering. Fire Research. Mechanical Systems. Organic Building Materials. Codes and Safety Standards. Heat Transfer. Inorganic Building Materials.

APPLIED MATHEMATICS. Numerical Analysis. Computation. Statistical Engineering. Mathematical Physics.

DATA PROCESSING SYSTEMS. Components and Techniques. Digital Circuitry. Digital Systems. Analog Systems. Applications Engineering.

ATOMIC PHYSICS. Spectroscopy. Radiometry. Mass Spectrometry. Solid State Physics. Electron Physics. Atomic Physics.

INSTRUMENTATION. Engineering Electronics. Electron Devices. Electronic Instrumentation. Mechanical Instruments. Basic Instrumentation.

Office of Weights and Measures.

BOULDER, COLO.

CRYOGENIC ENGINEERING. Cryogenic Equipment. Cryogenic Processes. Properties of Materials. Gas Liquefaction.

IONOSPHERE RESEARCH AND PROPAGATION. Low Frequency and Very Low Frequency Research. Ionosphere Research. Prediction Services. Sun-Earth Relationships. Field Engineering. Radio Warning Services.

RADIO PROPAGATION ENGINEERING. Data Reduction Instrumentation. Radio Noise. Tropospheric Measurements. Tropospheric Analysis. Propagation-Terrain Effects. Radio-Meteorology. Lower Atmosphere Physics.

RADIO STANDARDS. High frequency Electrical Standards. Radio Broadcast Service. Radio and Microwave Materials. Atomic Frequency and Time Standards. Electronic Calibration Center. Millimeter-Wave Research. Microwave Circuit Standards.

RADIO SYSTEMS. High Frequency and Very High Frequency Research. Modulation Research. Antenna Research. Navigation Systems. Space Telecommunications.

UPPER ATMOSPHERE AND SPACE PHYSICS. Upper Atmosphere and Plasma Physics. Ionosphere and Exosphere Scatter. Airglow and Aurora. Ionospheric Radio Astronomy.